Framework for Smart Transactive Energy in Home-Microgrids Considering Coalition Formation and Demand Side Management

Mousa Marzband[a,b,c,d], Mohammad Hossein Fouladfar[e], Mudathir Funsho Akorede[f], Gordon Lightbody[a,b], Edris Pouresmaeil[g]

[a]*Control and Intelligent Systems Group, Department of Electrical and Electronic Engineering, UCC, College Rd., Cork, Ireland*
[b]*SFI Research Centre for Marine and Renewable Energy, MaREI, Ireland*
[c]*Faculty of Engineering and Environment, Department of Maths, Physics and Electrical Engineering, Northumbria University Newcastle, Newcastle upon Tyne NE1 8ST, UK*
[d]*Dept. of Electrical Engineering, Lahijan branch, Islamic Azad University of Lahijan, Lahijan, Iran*
[e]*Dept. of Electrical Engineering, science and research of Bushehr Branch, Islamic Azad University, Bushehr, Iran*
[f]*Dept. of Electrical & Electronics Engineering, Faculty of Engineering and Technology, University of Ilorin, P.M.B. 1515, Ilorin, Nigeria.*
[g]*Dept. of Electrical Engineering and Automation, Aalto University, 02150 Espoo, Finland*

Abstract

The concept of Transactive energy (TE) been adapted in the regulation of electricity market within the context of economic planning and control for grid reliability enhancement. The objective is to improve productivity and participation of the players in the market that is composed of distributed energy resources (DER). The main goal of implementing a market structure based on TE is to secure permission for the market players so that they could attain a higher payoff. In this study, an optimization-based algorithm in which an objective function premised on economic strategies, distribution limitations and the overall demand in the market structure is proposed. The objective function is solved for near global optima using four heuristically guided optimization algorithms. The proposed algorithm which ensures that none of the independent players has priority and/or advantage over others, emphasizes optimum use of electrical/thermal energy distribution resources, while maximizing profit for the owners of the home Microgrids (H-MGs). Reduction in

Email address: `mousa.marzband@northumbria.ac.uk Corresponding author` (Mousa Marzband)

the market clearing price (MCP) for further participation and the response of the consumers′ responsive loads are also considered in the study. The feasibility of the proposed algorithm is validated in a coalition formation scenario among the existing H-MGs. Results show an increase in the profit attained, enhanced system reliability and a reduction in the electricity cost of the consumers.

Keywords: Transactive energy, home microgrids, coalition formation, responsive load, electricity market

---

Nomenclature

Acronyms

AEL	aggregated electrical load
ATL	aggregated thermal load
CHP	combined heat and power
DR	demand response
DR+, DR-	amount of responsive load demand (RLD) that goes/come from/to other time period to/from t
DW	dish washer
DER	distributed energy resources
DSO	distributed system operator
EES	electrical energy storage
ESP	electrical solar panel
EV	electrical vehicle
GB	gas boiler
HHW	heat and hot water
H-MG	home microgrid
MCP	market clearing price
MO-TE	market operator based on transactive energy
MG	Microgrid
NG	natural gas
PV	photovoltaic
REF	refrigerator

RET	retailer
RET+/RET-	buying/ selling power from/to H-MG *i*/ the retailer
SBP	system buy price
SSP	system sell price
SOC	state-of-charge
TD	thermal dump
TES	thermal energy storage
TSP	thermal solar panel
TE	transactive energy
Indices	
$E/\ h/\ t/i,\ i \in \{1, 2, \cdots, n\}$	electricity/ heat/ time steps/ H-MG number
$j \in$ {CHP, GB, TSP}	thermal DERs
$k \in$ {ESP, CHP}	electrical DERs
$m \in$ {DW, EV, REF, AEL}	electrical consumers
$p \in$ {HHW, ATL, TD}	thermal consumers
Constant values	
$\underline{\mathrm{SOC}}^{x}$, $\overline{\mathrm{SOC}}^{x}$, $\overline{\mathrm{P}}^{x}_{e/h}$, $\underline{\mathrm{P}}^{x}_{e/h}$	minimum values/ maximum SOC/ power during X charging and discharging mode
$x \in$ {ES+, ES-, EV+, EV-, TES+, TES-}	
$\mathrm{E}^{x}_{\mathrm{Tot}}$	total value of X capacity

$\underline{T}^{y}$, $\overline{T}^{y}$	maximum/ minimum value of y temperature
$y \in \{REF, HHW\}$	
$\overline{P}^{j}_{e/h}$, $\underline{P}^{j}_{e/h}$	minimum values/ maximum electrical thermal power j
T^{y}_{INI}, T^{RED}, T^{INC}	initial temperature/ the amount of temperature reduction each time the REF compressor is turned on/ the amount of temperature increase each time HHW is turned on
$\zeta^{j}_{e/h}$	electrical and thermal efficiencies *j*
$\underline{T}^{HHW}$, $\overline{T}^{HHW}$	maximum and minimum values of temperature
$\overline{E}^{x}$, $\underline{E}^{x}$	maximum and minimum values of energy in x
$\overline{E}^{x}$, $\underline{E}^{x}$	maximum and minimum values of z price bids
$z \in \{j,k,m,l\}$	
π^{NG}_{t}	natural gas price
Constant values	
$\tilde{\lambda}^{MCP}_{t}$	MCP prediction value during each time interval *t* (£/kWh)
Decision variables	
X^{Ret}_{t}, X^{ES}_{t}, X^{TES}_{t}, X^{DR}_{t}	binary variable of retailer, electrical energy storage, thermal energy storage, demand response
$P^{m}_{t,e}$, $P^{p}_{t,h}$	Consumed electrical/ thermal power by l/ m at time t
$P^{j}_{t,e}$, $P^{k}_{t,h}$	Electrical/ thermal power generated by k/ j at time t
$\pi^{z}_{t,e}$, $\pi^{z}_{t,h}$	Electrical/ thermal price bids by z at time t
$P^{Ret+,j}_{t,e}$, $P^{Ret-,j}_{t,e}$	The electric power sold/ bought by H-MG i to/from the retailer
$\lambda^{MCP}_{t,s}$	Market clearing price by using the S optimization method (£/kWh)
	S=1: particle swarm optimization (PSO)
	S=2: harmony search (HS)
	S=3: differential evolution (DE) algorithm
	S=4: bat algorithm (BAT)

1. Introduction

The ever-increasing global demand for electricity, coupled with the fast depletion of the fossil fuels, as well as the environmental impact of burning these fuels has led to the present restructured electricity industry [1]. The aforementioned factors have led to emergence of new technologies for generation, distribution, energy transfer and consumption as well as the need for optimum energy management and energy efficiency improvements [2–5]. To this end, smart grids, evolved from upgrading of the existing electricity grids with these new technologies and services which make them more reliable, optimal and environmentally friendly, have been proposed [6–9]. In contrast to the traditional power grids, smart grids are developing rapidly with a structure based on home microgrids (H-MG) with certain desirable features such as self troubleshooting and self repair, as well as comprehensive control [10, 11].

In developing smart grids, the concept of Transactive energy (TE) has become indispensable to enable further participation of different players in the power industry. This concept ensures the security of supply and reduces the need for exchange of personal information among the players [10–22]. Furthermore, TE is a combination of economic and control techniques with the aim of increasing the system efficiency and reliability.

The TE concept is also executable in non-concentrated electrical energy competitive markets [19]. One of the advantages of TE is that it allows the consumers to be supplied from any resource of their choice. The framework of the market structure includes drivers such as: 1) advancement in technology and customer knowledge, 2) need to enhance system productivity 3) depletion of the fossil fuels, 4) quest for more reliable and flexible systems, 5) need for a reduction in air pollution and, 6) further participation of the players in the market [10, 19, 23].

With the energy transfer concept, TE systems help grid reliability and improve both efficiency and interaction among system stakeholders [24]. The consumers' participation in the demand response (DR) load program has a significant role in the market structure based on TE since DR is one of the possible strategies to maintain a balance between the supply and demand in H-MGs. The DR program is designed to shift load demands away from system peak demand towards non-peak intervals. In [22], the effect of DR planning was investigated over the market dynamics based on price. The efficiency of the electricity market and the power grid was demonstrated in the study.

It was shown in [24, 25] that implementing DR also removes the problem of predicting flexible loads and the probability of the customer's response to price in the retail market. In the market structure based on TE, the retailers act as a bridge between wholesalers and small customers. On the other hand, the H-MGs are a part of the smart grid on the side of the consumer. H-MGs are considered as another active player in the market structure [26–32]. In the presence of electric vehicles (EV), the studies presented a non-concentrated control method in a bid to minimise the cost of the DERs in the H-MG to reduce the distribution power loss. In this method, a price coordinator was presented to assess the mutual effect of the distribution system operator (DSO) and the collectors in a smart grid.

In [33, 34], an H-MG incorporating a photovoltaic (PV) system showed the responsiveness of strategies to price for charging EV. While it increases the strength of short-term demand, it significantly reduces the costs of energy for the customers. A solution for the coordinated execution of DR in H-MG by learning the prediction of power demand based on life style and social-environmental factors was presented in [33]. The other important issue in a market based on the TE structure is the possibility of one player forming a coalition with other players. In [35] the H-MGs, both grid-connected and off grid configurations, participated in coalition with each other in a market structure. Simulation results showed significant reduction in power losses and a cost reduction in both modes. In [36], it was demonstrated that cooperative algorithms are approximately one hundred percent more profitable than non-cooperative algorithms. In the same vein, using coalition game theory to reduce the power loss in transfer lines, could lead to a reduction in the cost.

The following deficiencies regarding creation of an energy management system for multiple H-MGs based on TE concept have been identified from previous work and highlighted in this paper:

- Lack of an algorithm for exchange of energy and the impossibility of supplying the consumer load demand through the generating resources of other H-MGs [10, 11, 36–41];

- Non-availability of a demand response program to calculate the MCP [10, 11, 17–22, 35, 42–46].
- Non-existence of optimization algorithms for solving and implementing the optimum clearance of the market process and obtaining pay-off for all market players [18, 20, 34, 47, 48].
- Inability to determine the strategy and behaviour of residential customers as prosumer for participating in the market [21, 49–52].
- Lack of an algorithm to achieve the overall profit of the players and address the stochastic behaviour of the players in the optimization process [19, 33, 53–55].

In this paper, improved versions of the popular optimization techniques, including particle swarm optimization (PSO), harmony search (HS), differential evolution (DE) and the bat algorithm (BAT) are used to solve the non-linear and non-convex Market Operator Transactive Energy (MO-TE) structure problem. It is common knowledge that a simple optimization problem may not provide the level of robustness required for multiple H-MGs. In other words, the intricacy of tuning the parameters in optimization algorithms may not give the expected results in such cases. Since the proposed problem in this paper deals with a very large number of combinations and a wider search space, it demands a robust heuristic algorithm. The proposed optimization algorithm exploits the stochastic weight trade-off mechanism amongst previous velocity momentum, cognitive and social components using dynamic acceleration coefficients trade-off. This is done to maintain the balance between global and local exploitation, and results in an improved search capability of the algorithm. The incorporation of mechanisms to increase swarm members diversity through lethargy and freak factors could avoid swarm members from being trapped in local minima, thereby alleviating premature convergence which is associated with the conventional optimization algorithms in problems with multiple local optima.

A more accurate modeling of the MO-TE problem is carried out by considering the uncertainty in the inputs and network interaction. Appropriate coalition formation functions are incorporated in the fitness function to handle different equality and inequality constraints. The convergence and the solution quality of the proposed algorithms are affected by the selected acceleration coefficients; relatively high value of these components leads the particles to a local optimum, while relatively high values of cognitive components leads to wander of the particles over the search space. To improve the solution quality, these coefficients will be updated in a way that the cognitive component is reduced as the social component is increased with each iteration. The proposed optimization method has the flexibility to enhance both global and local exploration abilities. The results obtained are compared with one another and the outcome evaluations substantiate the applicability of the proposed optimization techniques for solving constrained electrical/thermal economic dispatch problems with non-smooth cost functions. The efficiency of the proposed algorithm is evaluated using a benchmark test-bed.

The contributions of this paper can be summarized as follows:

- Inclusion of neighbourhood grids for the players participating in the market pool. This model is a non-linear one capable of determining the optimum price bid for the power, generation and consumption resources when the players are inclined to form a coalition. For this purpose, a comprehensive mathematical model which can easily be generalized to other structures, is presented.

- A new formulation of the specific demand side management strategy for maximizing the total profit of the grid under study is carried out with the load demand and market clearing prices.

- An increase in pay-off resulting from the participation of the consumers in the TE structure due to their inclination to participate in the DR program.

- Proposition of a day-ahead scheduling model for a multiple smart H-MG system with the possibility of coalition formation. The problem is formulated to minimize the sum value of the overall generation cost while satisfying various constraints.

- Development of several hybrid optimization search algorithms with differential evolution to solve the complicated constrained optimization problems. The mutation and selection operations for differential evolution algorithms are also modified.

To verify the proposed day-ahead scheduling model and the solution technique, several test H-MG systems are employed on a real test under different fault scenarios.

The rest part of this paper is organized as follows:

Section 2 presents the structure of the proposed market while Section 3 gives an overview of the structure which includes the uncertainty unit, TE unit and MCP unit. The description of the power network under study, the objective function formulation as well as the problem constraints are presented in Section 5. While simulation results of the case study system are presented and discussed in Section 6, Section 7 concludes the paper.

2. Market Operator Transactive Energy (MO-TE) structure

The exchange of information and communication among different players involved in the MO-TE structure is shown in Figure 1. As observed in this figure, each H-MG contains dispatchable generation units (DGU) (such as diesel generator) and non-dispatchable units (NDU) (such as solar photovoltaic (PV) systems and wind turbine (WT)), energy storage resources (ES) such as battery, non-responsive loads (NRL) and responsive load demand (RLD). The RLD is a composite load which consists of domestic and commercial types of load, and which can be fully curtailed in accordance with the bilateral contracts signed by the H-MG owner/operator and the customers. Due to the presence of these classes of consumers, MO-TE gives an opportunity for the consumers to participate in the DR program to reduce cost.

As depicted in Figure 1, retailers sell electrical energy to the customers through the MO-TE structure. MO-TE encourages investors and DER owners to participate in the market by increasing the profit that results from forming a coalition in order to share the energy generated in each H-MG. It also encourages the consumers to follow the DR program.

3. Implementation of the MO-TE structure

A framework of an algorithm designed to increase the participation of the DERs in MO-TE in order to reduce electricity price, to increase the generator′s profit as well as to reduce consumer′s cost is presented in Figure 2. This framework is presented with a view to reducing the power in the equilibrium, managing the demand side optimally considering the possibility of forming coalition among the generators, and reducing the market clearing price. The MO-TE structure consists of three main units: the Taguchi orthogonal test (TOAT) unit, the TE unit and the MCP unit. As observed in Figure 2, the sunlight radiation data and the resulting generated PV power, the load demand, MCP, SBP and SSP are all considered as uncertainty parameters for each hour. The TOAT ensures that the testing scenarios provide good statistical information with a minimum number of tests, and significantly reduces the number of the testing burden. TOAT has been proven to have the ability to optimally select representative scenarios for testing all possible combinations. The MCP unit is presented to calculate the MCP value during each time period in a two-way tender system.

3.1. TOAT unit

The Taguchi orthogonal array test (TOAT) unit generates uncertainty scenarios along with the related probability of occurrence which considers the weather conditions of each NDU in the H-MG, as well as their power demands. This unit first performs the computation of the probability of the scenario created by selecting an orthogonal matrix for the existing uncertainties in the system and then creates n values for the load demand, MCP, SBP and SSP using a normal distribution and the radiation equation for the PV system.

TOAT approach has been used in a number of previous works. For example, references [56] and [57] employed it to obtain robust solutions in the production design of experimental problems. Further, the approach, with minimum number of scenarios insures that the experimental scenarios present good statistical information and reduces significantly the number of tests [58]. It has been proven that among all possible scenarios, TOAT has the capability to attain optimum result [59]. Compared with Monte Carlo method, TOAT provides far fewer test scenarios and

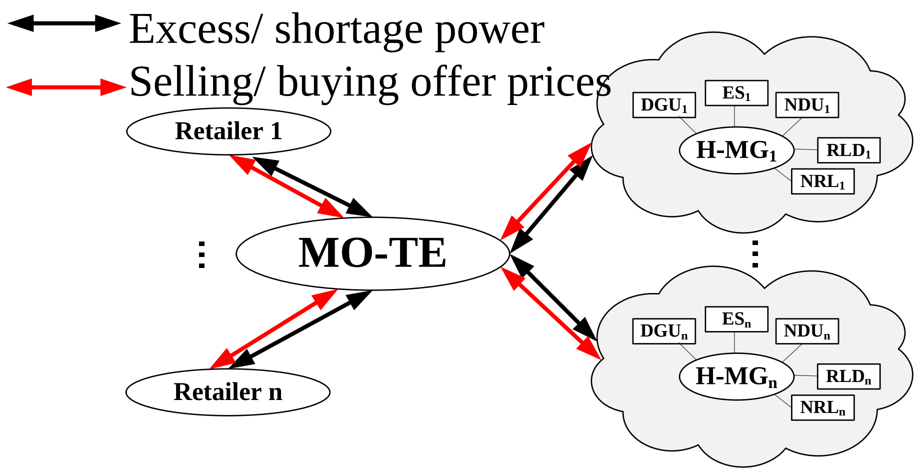

Figure 1: Exchange of information among the players in the TE structure

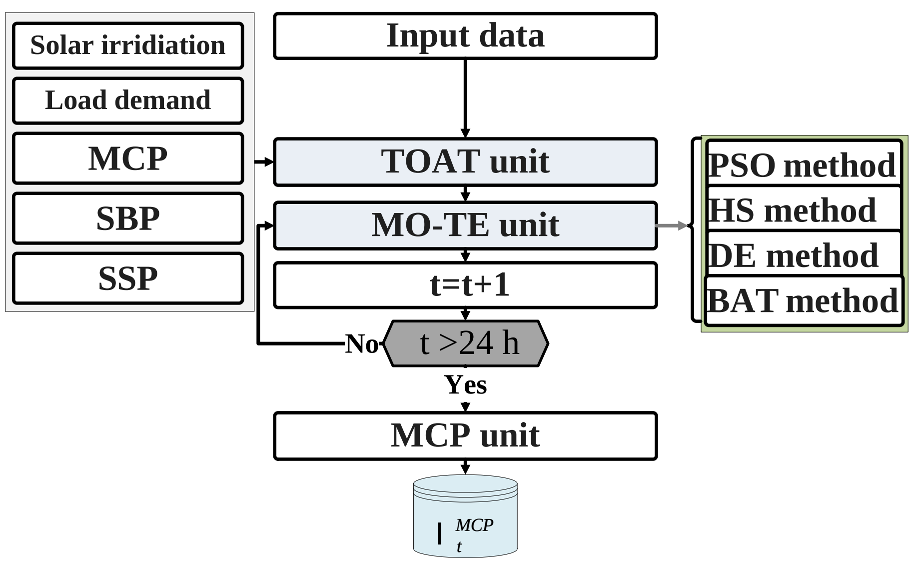

Figure 2: The proposed algorithm structure

leads to shorter computing time [60]. The method has be also employed in solving the load distribution and economic power dispatch problems in power systems [61].

The uncertainties in the problem and their associated scenarios implemented in the flowchart of Figure 3. This paper takes into account, the stochastic nature of renewable energy (solar power, wind power) penetration and load demand. An increase in the number of sources of uncertainty leads to an increase in the number of sensitivity analyses that need to be carried out, and hence extra terms will appear in the affine variables. If the uncertainty in the grid power is to be considered, then the sensitivity of nodal power injections to variations grid/slack bus power injection would be included in the noise terms of affine power-flow variables. However, the principle remains the same.

In addition, constraints are set by the retailer for limiting the grid trade. These constraints could be adjusted by the retailer during peak and off-peak hours, according to his discretion. It indirectly represents the extent to which the upstream grid can be relied on for power balance of the H-MG. In fact, the methodology does consider uncertainties, since: (a) it outputs flexible rules/schedules- not specific set-points for each actor of the H-MG and (b) it comes up with a merit-order dispatch list offering a fall-back, if the most profitable solution cannot be deployed. The uncertainty was accounted for by the forecast for each stochastic actor of the H-MG and covered by the multiple profitability levels. Further explanation regarding this unit can be found in [33] for interested readers.

3.2. TE unit

Methods for implementing the Transactive energy (TE) unit, such as particle swarm optimization (PSO), harmony search (HS), differential evolution (DE) and the bat algorithm (BAT) have been proposed by various researchers. For example, PSO is a population based evolutionary computational technique inspired by the social behaviour of flocking birds, where the velocity and position of the particles are updated to have additional components directed towards its own best position, and the overall best position [38]. PSO makes use of stochastic weight trade-off mechanism to maintain a balance between the global and local exploitation which improves the search capability. The diversity of swarm members is increased by using lethargy and freak factors to avoid avoid being trapped in local minima and thus premature convergence. In addition, the stochastic trade-off momentum control factor serves to adjust the quality of a candidate solution during the late search process [38].

The authors wish to stress that the stop criterion used in this work is not the maximum number of iterations, but rather an assessment of the information obtained from splitting any of the terminal nodes of the proposed optimization algorithms any further at that point. The proposed optimization algorithms do indeed replace the “bad quality” solutions with the “best” ones they find, and new solutions are generated using operators such as mutations and crossover. The infeasibility of infeasible solutions is determined by the unit commitment algorithm. If the unit commitment problem with the candidate optimal operation solutions cannot be solved, then new candidate values are generated. It is worth mentioning that there is no loss in performance when employing the de-centralized approach, as the methodology is platform independent. The iteration process is terminated if the best objective value is not improved for a certain number of iterations to avoid unnecessarily long iterations. To avoid premature stopping (while the objective function is still evolving when the maximum number of iterations occurs), the iteration count is increased until the objective value is no longer improved.

Figure 4 shows the flowchart for the TE unit. Each algorithm, which comprises electrical and thermal parts for the initial values of the variables as presented in Figures 4(a)- 4(c). As observed from Figure 4(a), should there be a power shortage in the electrical section, the CHP quickly swings into action to satisfy part of electrical power demand. In the event that the system suffers from further power shortage, then, there is the possibility of discharging the ES. It is worth mentioning that as the modelling of the ES and TES is very complex due to its specific nature, the authors have decided to solve it using four heuristic methods. The reason for this is to carry out a comparative analysis of the results from each one. The information system for the on-line dispatch can be prepared before obtaining the measured data. That is, the optimal power dispatch set points for all possible reserve requirements (corresponding to all possible uncertainties) can be made available in the database. This data which corresponds to the actual measured data (uncertainty/discrepancy) is selected and communicated to the local controllers in the second stage. In case the possibility of supplying part of the electrical charge demand does not exist, the unsupplied load demand is checked and shifted to another time period in which the value of MCP is much lower. Finally, if there is a power shortage, it is mostly compensated for by buying power through the retailers.

At some period, the excess generated electrical power is available in the H-MG under the conditions that the DR constraints are determined at the beginning of DR load demand; the ES is therefore exploited in charging mode. In case there is a shortage of thermal power, first the H-MG is brought into service and, if TES has the capability to discharge, it is discharged; otherwise it is bought from other H-MGs. However, if during each time interval, excess thermal power is available for each H-MG, TES is exploited in the charging mode while excess power generation continues The excess power is expended to supply a part of thermal power required by the other H-MGs.

The proposed algorithm does not necessarily use the lower, mean and upper values of each input variables. The lower and upper bounds are used to limit the decision variables to reasonable values. The algorithms each generate a set of candidate solutions, each containing a sizing value for each component. Each candidate solution is then evaluated using a fitness function, where the fitness is determined by a unit commitment based on mixed-integer linear programming that returns the operation cost. New solutions are generated by the proposed algorithms (based on the previous solutions, as for classical algorithms) until one of the stopping criteria is met. At the end of the process, the best solution is returned by the algorithm. This solution is the set of component sizes that returns the lowest total operation costs.

3.3. The MCP unit

In the electricity market, the generated/ consumed power of each generation and consumption resource and their proposed price are declared to the market operator. The energy generated in form of a stepwise function is sorted in ascending order while the amount of energy consumed is sorted in the shape of descending order. In this unit, as with the generators and consumers, the retailers also declare their offer price to buy and sell power. The final value of MCP is determined for the objective functions of each one of the market players in this unit. MCP will be the interaction between consumption and generation curves. Further explanations regarding this unit is presented by the authors in [33].

4. The advantages and disadvantages of each implemented optimization method

In this section, the advantages and disadvantages of each of the optimization methods implemented in this study are examined briefly.

- **PSO Method** [62–64]
  - **Advantages**
    - It has no overlapping and mutation calculation.
    - It is a zero order method which does not require complex mathematical operations such as taking partial derivatives.
    - Its rate of convergence is fast.
    - In contrast to other optimization methods, none of the particles (responses) are eliminated and only the value of each particle changes.
    - The elements have memory and each element maintains the effect of the best previous position.
    - It has a few parameters to handle.
  - **Disadvantages**
    - The efficiency of the algorithm reduces with increase in dimension
    - The method easily suffers from the partial optimism.

    * It requires more memory and this may cause it to slow down.
    * It cannot work out the problems of non-coordinate system.

- **DE Method** [65–67]
  - **Advantages**
    * It is capable of finding the true global minimum of a multimodal search space regardless of the initial parameter values.
    * It has fewer control parameters which makes it very powerful.
    * It is very easy to use.
    * Fast convergence.
  - **Disadvantages**
    * It is easy to drop into regional optimum.
    * It requires great ability to determine the optimal scale coefficient in order to reduce the search time.
    * Unstable convergence in the last period.

- **HS Method** [68, 69]
  - **Advantages**
    * In the genetic algorithm two chromosomes are used to generate a new chromosome or solution vector. In HS method all the exiting solution vectors are used in the memory to improvise new solution.
    * Its rate of convergence is fast.
    * It shows exceptional problem-solving ability.
  - **Disadvantages**
    * It can fall into local optima.
    * It is not efficient enough for solving large-scale problems, which has a slow convergence speed and low-precision solution [70].

- **BAT method** [71, 72]

- **Advantages**
  - it is much superior to other algorithms in terms of accuracy and efficiency [71].
  - It is relatively straightforward to implement in any programming language.
  - It can provide very quick convergence at a very initial stage by switching from exploration to exploitation.
  - It has flexible control parameters.
- **Disadvantage**
  - Implementation is more complicated than many other meta-heuristic algorithms [22]
  - It can fall in local optima.
  - it may lead to stagnation after some initial stage.

5. Problem formulation

The schematic of the grid under study is shown in Figure 5. The grid has n H-MGs of which the electrical and thermal DERs installed in them as well as their consumers are similar. In each one of the H-MGs, there exists the electrical and thermal stores and a set of generation resources such as GB, TSP, ESP, CHP as well as consumers comprising NRL and RLD. In this section, the problem formulation using the key components in the market structure based on Transactive Energy is presented. This framework is easily expandable for other electricity distribution systems with high levels of consumer participation.

5.1. Objective functions of the participants in MO-TE

The objective function based on maximization of the generator and retailers′ profits as well as the minimization of the consumers costs are formulated in Eq. 1, Eq. 2 and Eq. 3, respectively. The objective functions are non-linear in nature which can be solved for near global optima using four different heuristically guided algorithms. The effect of the large number of combinations of uncertainties on the computational speed does not matter since the first stage is for planning.

$$\begin{aligned} \max \sum_{\forall t}\sum_{\forall i}\sum_{\forall j}\sum_{\forall k}(\mathbb{R}_{t,e}^{k,i} + \mathbb{R}_{t,e}^{ES-,i} + \mathbb{R}_{t,h}^{j,i} + \mathbb{R}_{t,h}^{TES-,i} \\ -\mathbb{C}_{t,h}^{j,i} - \mathbb{C}_{t,h}^{TES+,i} - \mathbb{C}_{t,e}^{ES+,i} - \mathbb{C}_{t,e}^{k,i}) \times \Delta t \end{aligned} \tag{1}$$

$$\max \sum_{\forall t}\sum_{\forall i}(\mathbb{R}_{t,e}^{\text{Ret-},i} - \mathbb{C}_{t,h}^{\text{Ret-},i}) \times \Delta t \tag{2}$$

$$\min \sum_{\forall t}\sum_{\forall i}\sum_{\forall l}\sum_{\forall m}(\mathbb{C}_{t,h}^{p,i} + \mathbb{C}_{t,e}^{m,i}) \times \Delta t \tag{3}$$

where $\mathbb{R}_{t,e}^{k,i}$ and $\mathbb{R}_{t,h}^{j,i}$ are respectively the electrical and thermal revenue resulting from DERs k and j in H-MG i. $\mathbb{R}_{t,e}^{\text{ES-},i}$ and $\mathbb{R}_{t,h}^{\text{TES-},i}$ are respectively the revenue resulting from the ES and TES electrical and thermal discharge related to H-MG i at time t.

Also, $\mathbb{R}_{t,e}^{\text{Ret-},i}$ and $\mathbb{R}_{t,e}^{\text{Ret+},i}$ are respectively the revenue/ cost resulting from selling/ buying electrical power from/ to retailer H-MG i. $\mathbb{C}_{t,h}^{p,i}$ and $\mathbb{C}_{t,e}^{m,i}$ are respectively electricity costs related to p and m consumers at H-MG i.

5.2. Technical and economic constraints

5.2.1. Total electrical and thermal equilibrium

Deterministic constraints are imposed on the available and forecasted data of each DER unit, which are considered as inputs to the proposed technique. Furthermore, the inductive character of the rules of the proposed algorithm allows for flexibility when some probabilistic constraints (due to RES stochasticity) are reached. There is no need to train the system from actual data, which is one of the merits of the proposed optimization tool, provided that the forecasts and estimations for the data are realistic enough. The authors' previous work, which focused specifically on the tool ([34, 39, 73]) has clearly addressed this concern.

$$\begin{aligned} \sum_{\forall i}\sum_{\forall k}(P_{t,e}^{k,i} + P_{t,e}^{\text{ES-},i} + (1 - X_t^{\text{Ret}}) \cdot P_{t,e}^{\text{Ret-},i}) \\ = \sum_{\forall i}\sum_{\forall m}(P_{t,e}^{m,i} + P_{t,e}^{\text{ES+},i} + X_t^{\text{Ret}} \cdot P_{t,e}^{\text{Ret+},i}) \end{aligned} \tag{4}$$

$$\sum_{\forall i}\sum_{\forall j}(P_{t,h}^{j,i} + P_{t,h}^{\text{TES-},i} = \sum_{\forall i}\sum_{\forall l}(P_{t,h}^{p,i} + P_{t,h}^{\text{TES+},i}) \tag{5}$$

Eqs. (4) and (5) state that the total power generated by electrical/ thermal generators during each time interval, must be equal to the total demand of the electrical/ thermal consumers.

5.2.2. Retailer constraints

Eq. (6) shows the cost resulting from buying electrical power from the retailer into the H-MG i while Eq. (7) presents the retailer's offer price range for buying power into the H-MG i.

$$\mathbb{C}_{t,e}^{\text{Ret-},i} = \pi_{t,e}^{\text{Ret-},i} \times P_{t,e}^{\text{Ret-},i} \tag{6}$$

$$0 \leqslant \pi_{t,e}^{\text{Ret-},i} \leqslant \lambda_{t}^{\text{SBP}} \tag{7}$$

Also presented in Eq. (8) is the revenue resulting from selling electrical power from the H-MG i to the retailer, whereas Eq. (9) shows the price bid range for sales of power by the retailer to H-MG i.

$$\mathbb{R}_{t,e}^{\text{Ret+},i} = \pi_{t}^{\text{Ret+},i} \times P_{t,e}^{\text{Ret+},i} \tag{8}$$

$$0 \leqslant \pi_{t}^{\text{Ret+},i} \leqslant \lambda_{t,e}^{\text{SSP}} \tag{9}$$

Eqs. (10) and (11) show the exchanged power constraints between H-MG i and retailer.

$$P_{t,e}^{\text{Ret+},i} \leqslant X_{t}^{\text{Ret}} \times \overline{P}^{\text{Ret}} \tag{10}$$

$$P_{t,e}^{\text{Ret-},i} \leqslant (1 - X_{t}^{\text{Ret}}) \times \overline{P}^{\text{Ret}} \tag{11}$$

$$\overline{P}^{\text{Ret}} \leqslant (P_{t,e}^{\text{ESP},i} + P_{t,e}^{\text{CHP},i} + P_{t,e}^{\text{ES-},i}) \tag{12}$$

5.2.3. H-MG i constraints

ES and TES constraints in H-MG i

$$\mathbb{C}_{t,e}^{\text{ES+},i} = \pi_{t,e}^{\text{ES+},i} \times P_{t,e}^{\text{ES+},i} \tag{13}$$

$$0 \leqslant \pi_{t,e}^{\text{ES+},i} \leqslant \lambda_{t,e}^{\text{MCP}} \tag{14}$$

$$\mathbb{R}_{t,e}^{\text{ES-},i} = \pi_{t}^{\text{ES-},i} \times P_{t,e}^{\text{ES-},i} \tag{15}$$

$$0 \leqslant \pi_{t,e}^{\text{ES-}} \leqslant \lambda_{t,e}^{\text{MCP}} \tag{16}$$

where $\mathbb{C}_{t,e}^{\text{ES+,i}}$, $\mathbb{R}_{t,e}^{\text{ES-,i}}$, $\pi_{t,e}^{\text{ES+,i}}$ and $\pi_{t,e}^{\text{ES-,i}}$ respectively show the cost, revenue, and price bid resulting from buying/ selling electrical power by ES in H-MG i. Eqs. (17) to (19) present ES maximum and minimum charge/ discharge in H-MG i.

$$\underline{E}^{\text{ES,i}} \leqslant E_{t,e}^{\text{ES,i}} \leqslant \overline{E}^{\text{ES,i}} \tag{17}$$

$$P_{t,e}^{\text{ES-,i}} \leqslant \overline{P}^{\text{ES-,i}} \times X_{t}^{\text{ES,i}}, \quad P_{t,e}^{\text{ES-,i}} \geqslant 0 \tag{18}$$

$$P_{t,e}^{\text{ES+,i}} \leqslant \overline{P}^{\text{ES+,i}} \times X_{t}^{\text{ES,i}}, \quad P_{t,e}^{\text{ES+,i}} \geqslant 0 \tag{19}$$

Eqs. (20) and (21) are the charge/ discharge maximum limits for the energy in Eq. (22).

$$P_{t,e}^{\text{ES-,i}} \times \Delta t \leqslant (E_{t-1}^{\text{ES,i}} - \underline{E}^{\text{ES,i}}) \tag{20}$$

$$P_{t,e}^{\text{ES+,i}} \times \Delta t \leqslant (\overline{E}^{\text{ES,i}} - E_{t-1}^{\text{ES,i}}) \tag{21}$$

$$E_{t,e}^{\text{ES,i}} = E_{t-1,e}^{\text{ES,i}} + (P_{t-1}^{\text{ES+,i}} - P_{t-1}^{\text{ES-,i}}) \times \Delta t \tag{22}$$

Eq. (23) depicts the cost resulting from buying thermal power by TES in the charging mode while Eq. (24) is the price bid interval for buying thermal power by TES.

$$\mathbb{C}_{t,h}^{\text{TES+,i}} = \pi_{t,h}^{\text{TES+,i}} \times P_{t,h}^{\text{TES+,i}} \tag{23}$$

$$0 \leqslant \pi_{t,e}^{\text{TES+,i}} \leqslant \max(\pi_{t,h}^{\text{HHW,i}}, \pi_{t,h}^{\text{TD,i}}) \tag{24}$$

$\mathbb{R}_{t,h}^{\text{TES-,i}}$ in Eq. (25) is the revenue resulting from sales of thermal power generated by TES in the discharging mode and $\pi_{t,h}^{\text{TES-,i}}$ in Eq. (26) is the price bid variations range for selling thermal power by TES.

$$\mathbb{R}_{t,h}^{\text{TES-,i}} = \pi_{t,h}^{\text{TES-,i}} \times P_{t,h}^{\text{TES-,i}} \tag{25}$$

$$0 \leqslant \pi_{t,h}^{\text{TES-,i}} \leqslant \min(\max(\pi_{t,h}^{\text{CHP,i}}, \pi_{t,h}^{\text{GB,i}}), \pi_{t,h}^{\text{TSP,i}}) \tag{26}$$

In Eqs. (27) to (29), TES maximum and minimum charge/ discharge limitations are shown.

$$\underline{E}^{\text{TES,i}} \leqslant E_{t,h}^{\text{TES,i}} \leqslant \overline{E}^{\text{TES,i}} \tag{27}$$

$$P_{t,h}^{\text{TES-,i}} \leqslant \overline{P}^{\text{TES-,i}} \times X_{t}^{\text{TES,i}}, \quad P_{t,h}^{\text{TES-,i}} \geqslant 0 \tag{28}$$

$$P_{t,h}^{\text{TES+,i}} \leqslant \overline{P}^{\text{TES+,i}}, \quad P_{t,h}^{\text{TES+,i}} \geqslant 0 \tag{29}$$

Eqs. (30) and (31) show the discharge/ charge maximum limits for the energy in TES while Eq. (32) presents the energy equilibrium in TES.

$$P_{t,h}^{\text{TES-},i} \times \Delta t \leqslant (E_{t-1}^{\text{TES},i} - \underline{E}^{\text{TES},i}) \tag{30}$$

$$P_{t,h}^{\text{TES+},i} \times \Delta t \leqslant (\overline{E}^{\text{TES},i} - E_{t-1}^{\text{TES},i}) \tag{31}$$

$$E_{t,h}^{\text{TES},i} = E_{t-1,h}^{\text{TES},i} + (P_{t-1,h}^{\text{TES+},i} - P_{t-1,h}^{\text{TES-},i}) \times \Delta t \tag{32}$$

EV constraints in H-MG i

$$\text{if } X_t^{\text{EV},i} = 1 \Longrightarrow \underline{P}^{\text{EV+},i} \leqslant P_{t,e}^{\text{EV+},i} \leqslant \overline{P}^{\text{EV+},i} \tag{33}$$

Eq. (34) states that the $SOC_t^{\text{EV},i}$ of the automobile battery during each time interval related to H-MG i, must be less than its maximum value. It should be noted that Eq. (35) is the automobile battery power balance constraint. If EV is plugged out or once $SOC_t^{\text{EV},i}$ is reached to $\overline{SOC}^{\text{EV},i}$, then the charging process will be finished

$$SOC_t^{\text{EV},i} \leqslant \overline{SOC}^{\text{EV},i} \tag{34}$$

$$SOC_t^{\text{EV},i} = SOC_{t-1}^{\text{EV},i} - \frac{P_{t,e}^{\text{EV+},i} \times X_t^{\text{EV},i} \times \Delta t}{E_{\text{Tot}}^{\text{EV},i}} \tag{35}$$

$$\text{if } X_t^{\text{EV},i} = 0 \;\; \& \;\; SOC_t^{\text{EV},i} = \overline{SOC}^{\text{EV},i} \Longrightarrow P_{t,e}^{\text{EV+},i} = 0 \tag{36}$$

Eq. (37) is the cost of buying electrical power while Eq. (38) presents the offer price range for buying power by EV.

$$\mathbb{C}_{t,e}^{\text{EV+},i} = \pi_{t,e}^{\text{EV+},i} \times P_{t,e}^{\text{EV+},i} \tag{37}$$

$$0 \leqslant \pi_{t,e}^{\text{EV+},i} \leqslant \lambda_{t,e}^{\text{MCP}} \tag{38}$$

ESP constraints in H-MG i

The ESP generated power limitation is as shown in Eq. (39).

$$\underline{P}^{\text{ESP},i} \leqslant P_{t,e}^{\text{ESP},i} \leqslant \overline{\text{ESP}, i} \tag{39}$$

Eq. (40) shows the revenue resulting from generating electrical power by ESP whereas Eq. (41) shows the price bid range for selling power by ESP.

$$\mathbb{R}_{t,e}^{\text{ESP},i} = \pi_{t,e}^{\text{ESP},i} \times P_{t,e}^{\text{ESP},i} \tag{40}$$

$$0 \leqslant \pi_{t,e}^{\text{ESP},i} \times \lambda_{t,e}^{\text{MCP},i} \tag{41}$$

TSP constraints in H-MG i

Eq. (42) shows the generated thermal power income of TSP, and Eq. (43) shows the range of price bid for selling power by TSP.

$$\mathbb{R}_{t,h}^{\mathrm{TSP},i} = \pi_{t,h}^{\mathrm{TSP},i} \times P_{t,h}^{\mathrm{TSP},i} \tag{42}$$

$$0 \leqslant \pi_{t,h}^{\mathrm{TSP},i} \leqslant (\pi_{t,e}^{\mathrm{TES\text{-}},i}, \pi_{t,h}^{\mathrm{CHP},i}, \pi_{t,h}^{\mathrm{GB},i},) \tag{43}$$

CHP constraints in H-MG i

Eqs. (44)-(46) presents the power generation limitation for the CHP; where $FU_t^{\mathrm{CHP},i}$, $\zeta_{e1}^{\mathrm{CHP},i}$ and $\zeta h^{\mathrm{CHP},i}$ are respectively the fuel, electrical efficiency and thermal efficiency of the CHP.

$$\underline{P}^{\mathrm{CHP},i} \leqslant P_{t,e}^{\mathrm{CHP},i} \leqslant \overline{P}^{\mathrm{CHP},i} \tag{44}$$

$$P_{t,e}^{\mathrm{CHP},i} = FU_t^{\mathrm{CHP},i} \times \zeta_{e1}^{\mathrm{CHP},i} + \zeta_{e2}^{\mathrm{CHP},i} \tag{45}$$

$$P_{t,e}^{\mathrm{CHP},i} = \zeta_{e1}^{\mathrm{CHP},i} \times \frac{P_{t,h}^{\mathrm{CHP},i}}{\zeta h^{\mathrm{CHP},i}} + \zeta_{e2}^{\mathrm{CHP},i} \tag{46}$$

Eq. (47) is the cost resulting from power generation using CHP. Eq. (48) shows the price bid range for generating power by CHP. Also, Eqs. (49) and (50) state the revenue resulting from selling electrical and thermal powers generated using the CHP.

$$\mathbb{C}_t^{\mathrm{CHP},i} = \pi_t^{\mathrm{NG}} \times FU_t^{\mathrm{CHP},i} \tag{47}$$

$$\mathbb{C}_t^{\mathrm{CHP},i} \leqslant \pi_t^{\mathrm{CHP},i} \leqslant 2 \times \mathbb{C}_t^{\mathrm{CHP},i} \tag{48}$$

$$\mathbb{R}_{t,e}^{\mathrm{CHP},i} = \pi_{t,e}^{\mathrm{CHP},i} \times P_{t,e}^{\mathrm{CHP},i} \tag{49}$$

$$\mathbb{R}_{t,h}^{\mathrm{CHP},i} = \pi_{t,h}^{\mathrm{CHP},i} \times P_{t,h}^{\mathrm{CHP},i} \tag{50}$$

GB constraints in H-MG i

The limit of the power generated by GB is shown in Eq. (51).

$$0 \leqslant P_{t,h}^{\mathrm{GB},i} \leqslant \overline{P}_{t,h}^{\mathrm{GB},i} \tag{51}$$

Eq. (52) shows the cost resulting from generating thermal power by GB while Eq. (53) presents the amount of fuel consumed using GB and Eq. (54) shows the price bid range for selling power through GB.

$$\mathbb{C}_{t,h}^{\mathrm{GB},i} = \pi_{t,h}^{\mathrm{NG}} \times FU_t^{\mathrm{GB},i} \tag{52}$$

$$FU_t^{\mathrm{GB},i} = \frac{P_t^{\mathrm{GB},i}}{\zeta_h^{\mathrm{GB}}} \tag{53}$$

$$\mathbb{C}_{t,h}^{\mathrm{GB},i} \leqslant \pi_{t,h}^{\mathrm{GB},i} \leqslant 2 \times \mathbb{C}_{t,h}^{\mathrm{GB},i} \tag{54}$$

The revenue resulting from selling thermal power by GB is shown in Eq. (55).

$$\mathbb{R}_{t,h}^{\mathrm{GB},i} = \pi_{t,h}^{\mathrm{GB},i} \times P_{t,h}^{\mathrm{GB},i} \tag{55}$$

5.2.4. *Consumer constraints*

DR constraints

Eq. (56) shows that the value of shiftable power must be less than or equal to the difference of the total consumed power and the total generated power. Eq. (58) and Eq. (59) show that the DR limit between two consecutive intervals must not exceed a certain limit.

$$P_t^{\mathrm{DR\text{-}},i} \leqslant (P_t^{\mathrm{TCP},i} - P_t^{\mathrm{TGP},i}) \cdot X_t^{\mathrm{DR\text{-}},i} \tag{56}$$

$$P_t^{\mathrm{DR+},i} \leqslant (P_t^{\mathrm{TGP},i} - P_t^{\mathrm{TCP},i}) \cdot (1 - X_t^{\mathrm{DR\text{-}},i}) \tag{57}$$

$$P_t^{\mathrm{DR+},i} \leqslant k_\epsilon \times P_t^{\mathrm{NRL},i} \times (1 - X_t^{\mathrm{DR\text{-}},i}) \tag{58}$$

$$-k_t \leqslant (P_t^{\mathrm{DR+},i} - P_{t-1}^{\mathrm{DR+},i}) \leqslant k_t \tag{59}$$

ATL and AEL constraints

Eqs. (60) and (61) are the costs resulting from buying electric and thermal power by AEL and ATL. Also, Eqs. (62) and (63) present the price bid interval for buying power by AEL and ATL.

$$\mathbb{C}_{t,e}^{\mathrm{AEL},i} = \pi_{t,e}^{\mathrm{AEL},i} \times P_{t,e}^{\mathrm{AEL},i} \tag{60}$$

$$\mathbb{C}_{t,e}^{\mathrm{ATL},i} = \pi_{t,e}^{\mathrm{ATL},i} \times P_{t,e}^{\mathrm{ATL},i} \tag{61}$$

$$\lambda_{t,e}^{\mathrm{MCP}} \leqslant \pi_{t,e}^{\mathrm{AEL},i} \leqslant 2 \times \lambda_{t,e}^{\mathrm{MCP}} \tag{62}$$

$$\max(\pi_{t,h}^{\mathrm{TES\text{-}},i}, \pi_{t,h}^{\mathrm{CHP},i}, \pi_{t,h}^{\mathrm{GB},i}, \pi_{t,h}^{\mathrm{TSP},i}) \leqslant \pi_{t,h}^{\mathrm{ATL},i} \leqslant 2 \times \max(\pi_{t,h}^{\mathrm{TES\text{-}},i}, \pi_{t,h}^{\mathrm{CHP},i}, \pi_{t,h}^{\mathrm{GB},i}, \pi_{t,h}^{\mathrm{TSP},i}) \tag{63}$$

TD constraints

Eq. (64) is the cost of buying thermal power by TD while Eq. (65) states the offer price range for buying power by TD.

$$\mathbb{C}_{t,h}^{\mathrm{TD},i} = \pi_{t,h}^{\mathrm{TD},i} \times P_{t,h}^{\mathrm{TD},i} \tag{64}$$

$$0 \leqslant \pi_{t,h}^{\mathrm{TD},i} \leqslant \min(\pi_{t,h}^{\mathrm{TES\text{-}},i}, \pi_{t,h}^{\mathrm{CHP},i}, \pi_{t,h}^{\mathrm{GB},i}, \pi_{t,h}^{\mathrm{TSP},i},) \tag{65}$$

REF constraints

Eqs. (66)-(70) state the modeling of REF. $\mathbb{C}_{t,e}^{\mathrm{REF},i}$ is the cost resulting from buying power by REF and $\pi_{t,e}^{\mathrm{REF},i}$ represent the offer price interval for buying power.

$$\begin{cases} \text{if } \underline{T}^{\mathrm{REF},i} \leqslant T_t^{\mathrm{RET}} \leqslant \overline{T}^{\mathrm{REF},i} & X_t^{\mathrm{REF},i} = 1 \\ \text{Otherwise} & X_t^{\mathrm{REF},i} = 0 \end{cases} \tag{66}$$

$$X_t^{\mathrm{REF},i} = 1 \Longrightarrow P_{t,e}^{\mathrm{REF},i} = \overline{P}^{\mathrm{REF},i} \quad \& \quad T_t^{\mathrm{REF},i} = T_{t-1}^{\mathrm{REF},i} - T^{\mathrm{RED},i} \tag{67}$$

$$X_t^{\mathrm{REF},i} = 0 \Longrightarrow P_{t,e}^{\mathrm{REF},i} = 0 \quad \& \quad T_t^{\mathrm{REF},i} = T_{t-1}^{\mathrm{REF},i} + T^{\mathrm{RED},i} \tag{68}$$

$$\mathbb{C}_{t,e}^{\mathrm{REF},i} = \pi_{t,e}^{\mathrm{REF},i} \times P_{t,e}^{\mathrm{REF},i} \tag{69}$$

$$0 \leqslant \pi_{t,e}^{\mathrm{REF},i} \leqslant \lambda_{t,e}^{\mathrm{MCP}} \tag{70}$$

DW constraints

The modeling of DW are presented in Eqs. (71)-(74). Eqs. (73) and (74) respectively show the cost resulting from buying power by DW and the price bid interval for buying power.

$$\text{if } X_t^{\mathrm{DW},i} = 1 \Longrightarrow P_{t,e}^{\mathrm{DW},i} = \overline{P}^{\mathrm{DW},i}, \quad DT_t^{\mathrm{DW},i} = DT_{t-1}^{\mathrm{DW},i} + 1 \tag{71}$$

$$\text{if } DT_t^{\mathrm{DW},i} = \overline{DT}^{\mathrm{DW},i} \Longrightarrow P_{t,e}^{\mathrm{DW},i} = 0, \quad X_t^{\mathrm{DW},i} \tag{72}$$

$$\mathbb{C}_{t,e}^{\mathrm{DW},i} = \pi_{t,e}^{\mathrm{DW},i} \times P_{t,e}^{\mathrm{DW},i} \tag{73}$$

$$0 \leqslant \pi_{t,e}^{\mathrm{DW},i} \leqslant \lambda_{t,e}^{\mathrm{MCP}} \tag{74}$$

HHW constraints

The modeling of HHW are presented in Eqs. (75)-(79).

$$\begin{cases} \text{if } \underline{T}^{\mathrm{HHW},i} \leqslant T_t^{\mathrm{HHW}} \leqslant \overline{T}^{\mathrm{HHW},i} & X_t^{\mathrm{HHW},i} = 0 \\ \text{Otherwise} & X_t^{\mathrm{HHW},i} = 1 \end{cases} \tag{75}$$

$$X_t^{\mathrm{HHW},i} = 1 \Longrightarrow \begin{cases} P_{t,e}^{\mathrm{HHW},i} = \overline{P}^{\mathrm{HHW},i} \\ T_t^{\mathrm{HHW},i} = T_{t-1}^{\mathrm{HHW},i} + T^{\mathrm{INC},i} \end{cases} \tag{76}$$

$$X_t^{\mathrm{HHW},i} = 0 \Longrightarrow \begin{cases} P_{t,e}^{\mathrm{HHW},i} = 0 \\ T_t^{\mathrm{HHW},i} = T_{t-1}^{\mathrm{HHW},i} - T^{\mathrm{INC},i} \end{cases} \tag{77}$$

$$\mathbb{C}^{\mathrm{HHW},i}_{t,h} = \pi^{\mathrm{HHW},i}_{t,h} \times \mathrm{P}^{\mathrm{HHW},i}_{t,h} \tag{78}$$

$$0 \leqslant \pi^{\mathrm{HHW},i}_{t,h} \leqslant \max(\pi^{\mathrm{TES\text{-}},i}_{t,h}, \pi^{\mathrm{CHP},i}_{t,h}, \pi^{\mathrm{GB},i}_{t,h}, \pi^{\mathrm{TSP},i}_{t,h},) \tag{79}$$

5.3. Mathematical modelling of PV, WT and load demand uncertainty

Since the market is based on predicted data and generation units are variable, uncertainty must be considered. In order that the predicted data mimics reality, probabilistic models are used.

5.3.1. Modelling of load demand uncertainty

Load uncertainty can be modelled using a normal distribution curve. The mean value in the load normal curve distribution is equal to the predicted load for each time interval. The standard deviation is obtained from the load prediction method based on experience and previous electricity consumption patterns. To simplify our analysis, the normal distribution can be divided into several sections showing the load occurrence probability with the value equal to the mean value of that section. In this study the normal probability distribution curve shown in Figure 6 is used [74, 75].

5.3.2. WT uncertainty modelling

Bearing in mind that wind supply is stochastic in nature, the calculation of wind speed variability was carried out using the Weibull distribution. The mean value of this distribution is the wind speed prediction datum. The Weibull distribution curve can also be divided into several separate sections. The possibility of occurrence of each interval is determined from the corresponding wind speed and the mode of each section. The wind speed probability distribution curve in this study is divided in the five pieces distribution density function as shown in Figure 7 [76, 77].

Wind output power is determined from the power function based on wind speed according to the following relation.

$$P_t^{WT}(v) = \begin{cases} (\frac{P_r}{V_r - V_{ci}})(v - V_{ci}) & \text{if } V_{ci} \leqslant v \leqslant V_r \\ P_r & \text{if } V_r \leqslant v \leqslant V_{co} \\ 0 & \text{others} \end{cases} \tag{80}$$

where $P_t^{WT}(v)$ is total wind power output at wind speed v, v is the wind speed, P_r is total rated power of wind turbines, V_r is the rated wind speed and V_{ci} turbine cut-in wind speed and V_{co} is the cut-out wind speed. If the turbine generation starts at the speed V_{ci}; the output power will increase proportionally to speed increase from V_{ci} to V_r and the nominal power P_r is generated when the wind speed is varied between V_r and V_{co}. For security reasons, the turbine will turn off at speed V_{co} and the output power will be zero at a speed outside the mentioned limits.

5.3.3. Modelling of uncertainty in PV system

The amount of solar radiation that reaches the earth, in addition to the external daily and annual rotation of the sun, depends on the geographical position (length, width and height) and climatic conditions (for example cloud cover). The PV output power is dependent on the amount of solar radiation on the PV panel surface. The hourly distribution for solar radiation can be divided into five sections similar to the Weibull distribution model for wind speed, as illustrated in Figure 8 [78]. PV system power distribution is obtained based on the radiation distribution. The PV system output power is calculated as follows:

$$P_t^{PV} = A_C \cdot \eta \cdot I_t^{\beta} \tag{81}$$

where A_C is the area of array surface [m^2], I_t^{β} is the amount of solar radiation over a surface with β slope to the horizon surface [kWm^{-2}], η is the efficiency of PV system at the realistic reporting conditions.

6. Results and discussion

In this section, the results of simulation of the four methods are presented and discussed. The grid under study has three H-MGs called A, B and C which include different DER and consuming resources. The specifications of these resources are listed in the appendix. A fault on a H-MG will cause serious consequences to the system and customers' equipment. It requires not only concentrated attention to avoid the fault but also recovery measures to reduce the impact once the fault has occurred. Constructing a re-configurable scheme for different fault modes will greatly reduce losses and inconvenience. Hence, the proposed optimization algorithm is employed to solve the optimal day-ahead scheduling problem under different fault scenarios, to help verify the robustness of the algorithm.

The proposed methodologies provide a number of possible dispatch combinations. Hence, there is a large number of fallback positions that the optimization algorithm can revert to in the case of any imbalance. When an intra-period imbalance occurs, the next most suitable dispatch is applied immediately. A 1-hour resolution rolling-horizon simulation is used to verify the validity of the obtained scheduling solutions. It also helps to adjust the operation scheduling values if required, especially as the proposed optimization algorithm input data use a 1-day resolution to improve computation speed. Simulations were carried out on an Intel ® CoreTM: 5-3320M CPU @2.6GHz computer with 4:00GB RAM. The MATLAB software was used to solve the optimization problems.

It is worth mentioning that there are no infeasible dispatches in the problem. A solution/dispatch is considered infeasible if it cannot be realized in real time. The proposed optimization methodologies will produce a number of profitable dispatches at various profitability levels when it is executed in the hour-ahead horizon. However, in real time, it is possible that due to considerable deviations from the forecast, the schedule of the highest profitability may prove to be infeasible; hence the next best profitable schedule will be applied. This method outperforms previous approaches specifically in terms of outputting flexible schedules that cater for the mitigation of deviations of a H-MG. It also takes into account the risk of infeasible solutions through a merit order list of alternative dispatches.

The values of all the powers generated by electrical and thermal DERs in each H-MG as well as the total value of electrical powers sold/ bought to/ from H-MGs from/ to retailer are shown in Figure 9. As observed in Figure 9(a), the maximum power generated by the electrical DERs in H-MG #A is obtained by the HS method. This is why no power is sold from this H-MG to the retailer. For any uncertainty less than or equal to the maximum uncertainty, the corresponding reserve can be directly fetched from the uncertainty versus reserve information. This reduces the computational time of dynamic dispatch to approximately zero (around 0.1ms) due to the absence of recalculation of optimal power-flow for the measured data. The execution time will be the time taken for data selection, fetching and communication only.

In the proposed method, the sum of the power allocated to DR+ has the least value relative to other methods. The reason for the increase in the amount of generated power in this H-MG is to allow it to sell the generated power to other H-MGs. In this manner, the amount of H-MG #A revenue increases. As for H-MG #B, the conditions are completely different because the power generated using the DE method is higher than that for other methods. The reason for this is basically due to the power purchased from the retailer.

Overall, by comparing Figure 9(b) and 9(c), it is observed that H-MG #B in the PSO optimization method has a better interaction with the retailer compared to other methods. Bearing in mind that the average value of electrical MCP using the PSO method is lower than for other methods, H-MG #B supplies the number of consumers with lower MCP using the power purchased from the retailer. Furthermore, it is worth noting that the value of the DR+ power sum using this method is 27% of the total consumed DR+ power using other optimization methods. This means that in the MO-TE structure, the HS method attempts to buy more power from the retailer in order to supply more RLD loads. As observed in Figure 9(a) in H-MG #C the value of total power generated using the BAT method is highest compared to other optimization methods.

Similarly, from Figures 9(b) and 9(c), the power exchange value of the H-MG with the retailer has its highest limit in this method. The main reason for this is that the value of sum DR- has reached its lowest possible limit compared to other methods which is only 6%. On the other hand, about 26% of the total DR+ power was obtained with the BAT method. This figure is very significant when compared to the other methods. Knowing that the average value of electrical MCP in the BAT method is lower than the HS and DE methods, provides positive opportunities for supplying the consumers of this H-MG at lower price.

The total power generated by the thermal DER for each H-MG is shown in Figure 9(d). As observed in H-MGs #A and #C, the highest thermal power is generated by the HS method, whereas H-MG #B power is generated using the BAT method. In essence, the average value of thermal MCP using HS and BAT methods is lower than those for other methods. This information is very important to select further power generation by thermal DER resources. In other words, while the minimum value of thermal MCP is obtained in these methods, the maximum value of thermal MCP is obtained in the DE and PSO methods which could lead to a significant increase in the value of thermal power cost generated by these methods. As a result, less thermal power generated by the DE and PSO methods leads to a profit increase for the H-MG owner. Meanwhile the consumer that required maximum total thermal power has also been fulfilled.

Figure 10 presents the consumed load demand profile in each H-MG. It can be seen Figure 10(a) that the consumption peak value using the PSO and BAT methods in H-MG #A was shifted to non-peak intervals. Using the fact that the average MCP value during peak intervals is high in all the implemented optimization methods, then the participation of consumers in DR program incurs more expenses to H-MGs owners and/ or retailers in exchange for the supply of its required power. However, the total value of DR+ in the BAT method is about 28% of the total value of DR+, it is expected that the PSO method follows a similar pattern regarding participation of consuming resources to increase the DR+ value. After evaluation, it is observed that about 26% of the DR+ generation among the methods was obtained with PSO.

Despite this fact, it is observed that the total values of DR- in the DE and BAT methods are equal to each other, which is about 28% of the total DR- proposed by all the methods. The minimum value of total DR- was obtained from the HS method. This shows the reluctance of this method to shift the load demand from one time period with high price to another with lower price. The main reason for this occurrence is that the value of electricity generation cost by the H-MGs altogether has the highest value for all the methods. This is about a 28% reduction relative to the DE method that is providing the lowest cost of generating electricity. Using the HS method, H-MG #B has the maximum value of DR+ while DR- shows a significant reduction in its value.

As for the maximum electricity generation cost, the proposed algorithm shows a greater desire to reduce the value of the consumed load demand in the H-MG. An important point to make here is that although the electricity generation value in the BAT method was the highest after HS, the total value of DR- has become the lowest relative to other methods. For this reason, the BAT method has increased the DR+ value. In H-MG #C, DR+ and DR- values are maximum relative to other methods using the PSO method. The performance of this method is justified with its lowest cost of electricity after the DE method.

In H-MG #C, it is highly desirable that more DR+ be supplied using the BAT method while bringing DR- value to the minimum as was pointed out before. The electricity generation cost in the BAT method is high, as also is the average electrical MCP value compared to other methods during the 24h performance of the grid under study; by supplying the DRs at suitable times, the method therefore tries to reduce the cost paid by the consumers.

The percentage of the electrical power generated by the H-MGs for each optimization technique adopted in this study is shown in Figure 11 while that of thermal power is shown in Figure 12.

The thermal power supply required by the consumer is similar to that of electrical power. Therefore, the thermal power equilibrium for each H-MGs can be attained by implementing the optimization algorithms. Because supply of thermal power makes the thermal power GB resource to participate in each one the H-MGs. It should be noted that part of the thermal power is supplied by the GB which is brought in operation during the period 16:00-20:00. The pricing strategy by each of presented optimization methods somehow determines the suitable price offer for the GB during the period in which the CHP thermal power value is proportional to the electrical power. As a result, the thermal load requirement difference is satisfied by the GB.

The values of electrical and thermal MCPs obtained from simulation using each of the optimization methods are shown in Figures 13(a) and 13(b), respectively. As observed from Figure 13(a), all the methods for reducing electrical MCP relative to thermal MCP have very good performance over the complete time period. At the start of the system's daily performance, the PSO method has a better performance in reducing the MCP relative to the BAT method which during this time interval has the poorest performance. In the morning, the PSO method is the most successful for reducing the MCP. During this time interval the worst is related to the HS method for which the electrical MCP increases for about 83%.

HS performance over this latter time period is the worst among all the methods, so much so that it has out-weighed its very good performance at the beginning of the day. The PSO method in this interval obtains less MCP value relative to DE with about 34% of the time during the DERs and consumers proper management. Although PSO has shown the best performance during this time interval, it has the worst performance in the period from afternoon to sunset. The best performance to reduce MCP in this period from afternoon to sunset HS method which has obtained the minimum value of electrical MCP at about 78% of the time when compared with PSO.

During the day′s last hours, the HS method imposes a higher value of MCP on the consumers for 22% of the time. Altogether, the best method over the 24h performance of the MO-TE structure is obtained for electrical MCP using the HS method relative to the PSO method. This is about 6%, relative to BA, about 9% relative to the DE method; about 62% of the time a reduced MCP is obtained. As observed from Figure 13(b), at the beginning, from midnight until morning, the PSO method has a significant share in reducing the value of the thermal MCP. For this reason, its value is always obtained relative to other optimization methods at minimum value.

The worst result during this time interval is related to BAT where for about 77% of the time, a higher thermal MCP value results from using the PSO method. In the morning, the best performance is given by DE but the PSO′s performance has reduced so much that there is a reduction in the thermal MCP for about 45% of the time. In the time interval 12:00 to 18:00 the DE method gave the best performance. In contrast to DE, BAT had a poor performance whose operation is related to DE that was 70% weaker. During the last hours of the day in contrast to the previous intervals, BAT had the best performance relative to others. Altogether, for the powers consumed in all the H-MGs, the DE algorithm with less than 2% had better performance relative to BAT, 28% better relative to HS and PSO in reducing the MCP.

The convergence characteristic of the proposed algorithms is compared with each other and depicted in Figure 14. This figure implies that the proposed algorithm based on the DE method outperforms the other optimization techniques in convergence speed; however the proposed algorithm based on BAT method achieved a better performance from an optimality of objective function point of view. The obtained maximum profit for DE and BAT methods are £8.5 and £9.7, with the corresponding CPU-time of 8.085s and 9.705s (as shown in Table 1), respectively. It can be observed that the PSO method converges to the optimal solution in a greater number of iterations. It is observed from this figure that HS has a better convergence characteristic, in comparison with PSO and BAT. By comparing the convergence properties of the proposed algorithms, both the speed and ability of the proposed approaches to find better solutions can be observed in Figure 14. These imply the capability of the proposed methods for solving such complicated economic dispatch problems. The maximum iteration number for this case is set to 100 iterations.

In order to compare the computation, it should be mentioned that both CPU speed and simulation times for all methods are provided in Table 1. Computation time has a direct relation with CPU speed. Relative simulation time is calculated by multiplying relative CPU speed by the reported simulation time. Although the obtained profit by PSO is £7.9 (i.e., 22.6%) less than the profit obtained by BAT, but the corresponding CPU-time is much less in comparison with the very high CPU-time of BAT. The negligible reduction of profit at the expense of a significant increase of CPU-time may not be desirable from the real-time operation perspective. In it important to mention that in real-time applications, the optimal DER schedule is needed for the next few minutes, subject to the unpredicted uncertainty parameters in the order of minutes (e.g., 5-min intervals). The results presented in Table 1 substantiate the fact that the proposed methods are well capable of attaining the optimal solution of offer prices and quantities in a very short time. Hence, the proposed methods are efficient for solution of economic dispatch in real-time environment.

Table 1: Comparison of the absolute and relative CPU time for test system

Method	CPU speed (GHz)	Absolute time (s)	Relative CPU time (s)
DE	3	5.39	8.085
HS	3	5.33	7.995
PSO	3	5.26	7.89
BAT	3	6.47	9.705

Table 2 show the minimum, average, maximum and standard deviation of the objective function for different numbers of trial runs. The maximum iteration number for this simulation is selected to be 100. The results justify the applicability of the proposed methods for solving the constrained economic dispatch problem with non-smooth cost functions.

Table 2: Analysis of objective function for different number of trial runs

Method	Number of runs	Minimum profit (£)	Average profit (£)	Maximum profit (£)	Standard deviation (£)
DE	50	4.87	6.16	7.5	0.98
HS		3.6	7.14	7.64	1.23
PSO		4.66	6.15	6.98	0.93
BAT		4.83	6.81	8.4	1.34
DE	100	5.87	8.16	8.5	0.78
HS		4.6	8.34	8.84	1.03
PSO		5.66	7.15	7.9	0.56
BAT		5.93	7.93	9.7	1.23

7. Conclusion

This paper has proposed an algorithm for the optimum use of the existing electrical/ thermal resources in home Microgrids. The proposed framework provided an optimum timing for power exchange among the H-MGs while satisfying the objective functions and technical constraints. Establishing a coalition among the H-MGs, the method when tested, considered power balancing, demand side management, market clearing price reduction and profit increase of the players in the market. The optimality of the obtained results and the ability of the proposed structure to change the input parameters were compared with each other using several methods. With technical and economic constraints, the timing of connection of appliances and electrical machines were included. The optimum control of ES resources and demand side management led to a reduction in the exploitation cost of each H-MG which resulted in profit increase. The proposed algorithm could be exploited to fix different structures with different objective functions.

8. Acknowledgements

The authors acknowledge the fruitful discussions on game theory and H-MG interoperability with Prof. Jovica Milanovic from School of Electrical and Electronic Engineering, University of Manchester, Ferranti Building, M13 9PL Manchester, UK. This work was partly funded by European Union's Horizon 2020 research and innovation programme (NobelGrid project) under the grant agreement # 646184.

Credence. US-Ireland Research and Development Partnership Program (centre to centre), funded by Science Foundation Ireland (SFI) and The National Science Foundation (NSF) under the grant number 16/US-C2C/3290 is gratefully acknowledged.

Appendix

H-MG resources specifications and constant parameter values is listed in Table 3.

References

[1] M. V. Ramesh, A. R. Devidas, A. K., V. Rangan, Using CPS enabled microgrid system for optimal power utilization and supply strategy, Energy and Buildings 145 (2017) 32–43.

Table 3: H-MG resources specifications and constant parameter values

Name of DER	Variable	Value	Name of DER	Variable	Value
GB	ζ_{h}^{GB} $\overline{P}_{h}^{GB}$ $\underline{P}_{h}^{GB}$	85% 12 3.6	ES	$\overline{P}_{t,e}^{ES+}$ $\underline{P}_{t,e}^{ES+}$ $\overline{P}_{t,e}^{ES-}$ $\underline{P}_{t,e}^{ES-}$ $\underline{P}_{t,e}^{ES-}$ $\underline{SOC}^{ES}$ $\overline{SOC}^{ES}$	30 0.34 30 0.34 0.34 0 100%
CHP	ζ_{e2}^{CHP} ζ_{e1}^{CHP} $\overline{P}_{e}^{CHP}$ $\underline{P}_{e}^{CHP}$	-94.6916 0.358511 8 2	EV	$\overline{P}_{t,e}^{EV+}$ $\underline{P}_{t,e}^{EV+}$ $\underline{SOC}^{EV}$ $\overline{SOC}^{EV}$	3.2 0 0 100%
DW	$\overline{P}^{DW}$	0.42	REF	$P_{t,e}^{REF}$ $\overline{T}^{REF}$ $\underline{T}^{REF}$ T_{INI}^{REF} T^{INI}	0.12 9 3 27 6
HHW	$\overline{P}_{t,e}^{HHW}$ T_{INI}^{HHW}, $\underline{T}^{HHW}$ T^{INC} $\overline{T}^{HHW}$	0.5 18 6 36			
Natural gas	π_{t}^{NG}	0.0120760	TES	$\overline{P}^{TES+}$ $\underline{P}^{TES+}$ $\overline{P}^{TES-}$ $\underline{P}^{TES-}$	14.4 0 14.4 0
DR	k_{ϵ} k_{t}	5 5			

[2] T. AlSkaif, A. C. Luna, M. G. Zapata, J. M. Guerrero, B. Bellalta, Reputation-based joint scheduling of households appliances and storage in a microgrid with a shared battery, Energy and Buildings 138 (2017) 228–39.

[3] H. Chitsaz, H. Shaker, H. Zareipour, D. Wood, N. Amjady, Short-term electricity load forecasting of buildings in microgrids, Energy and Buildings 99 (2015) 50–60.

[4] Z. Zeng, R. Zhao, H. Yang, Micro-sources design of an intelligent building integrated with micro-grid, Energy and Buildings 57 (2013) 261–67.

[5] M. Sechilariu, B. Wang, F. Locment, Building-integrated microgrid: Advanced local energy management for forthcoming smart power grid communication, Energy and Buildings 59 (2013) 236–43.

[6] Y. Wang, B. Wang, C.-C. Chu, H. Pota, R. Gadh, Energy management for a

commercial building microgrid with stationary and mobile battery storage, Energy and Buildings 116 (2016) 141–50.

[7] E. Shirazi, S. Jadid, Optimal residential appliance scheduling under dynamic pricing scheme via hemdas, Energy and Buildings 93 (2015) 40–49.

[8] D. Balić, D. Maljković, D. Lončar, Multi-criteria analysis of district heating system operation strategy, Energy Conversion and Management 144 (2017) 414–28.

[9] S. Nojavan, M. Majidi, A. Najafi-Ghalelou, M. Ghahramani, K. Zare, A cost-emission model for fuel cell/pv/battery hybrid energy system in the presence of demand response program: e-constraint method and fuzzy satisfying approach, Energy Conversion and Management 138 (2017) 383–92.

[10] I. Dusparic, C. Harris, A. Marinescu, V. Cahill, S. Clarke, Multi-agent residential demand response based on load forecasting, in: 2013 1st IEEE Conference on Technologies for Sustainability (SusTech), 2013, pp. 90–96.

[11] Q. Ren, L. Bai, S. Biswas, F. Ferrese, Q. Dong, Demand-supply balancing using multi-agent system for bus-oriented microgrids, in: 2015 Resilience Week (RWS), 2015, pp. 1–8.

[12] F. Calise, R. D. Figaj, L. Vanoli, A novel polygeneration system integrating photovoltaic/thermal collectors, solar assisted heat pump, adsorption chiller and electrical energy storage: Dynamic and energy-economic analysis, Energy Conversion and Management (2017) –.

[13] L. Yu, Y. Li, G. Huang, C. An, A robust flexible-probabilistic programming method for planning municipal energy system with considering peak-electricity price and electric vehicle, Energy Conversion and Management 137 (2017) 97–112.

[14] W. Fang, Q. Huang, S. Huang, J. Yang, E. Meng, Y. Li, Optimal sizing of utility-scale photovoltaic power generation complementarily operating with

hydropower: A case study of the world's largest hydro-photovoltaic plant, Energy Conversion and Management 136 (2017) 161–72.

[15] S. I. Garcia, R. F. Garcia, J. C. Carril, D. I. Garcia, Critical review of the first-law efficiency in different power combined cycle architectures, Energy Conversion and Management 148 (2017) 844–59.

[16] S. Baldi, T. L. Quang, O. Holub, P. Endel, Real-time monitoring energy efficiency and performance degradation of condensing boilers, Energy Conversion and Management 136 (2017) 329–39.

[17] S. Behboodi, D. P. Chassin, C. Crawford, N. Djilali, Electric vehicle participation in transactive power systems using real-time retail prices, in: 2016 49th Hawaii International Conference on System Sciences (HICSS), 2016, pp. 2400–07.

[18] A. Ipakchi, Demand side and distributed resource management- a transactive solution, in: 2011 IEEE Power and Energy Society General Meeting, 2011, pp. 1–8.

[19] H. N. Aung, A. M. Khambadkone, D. Srinivasan, T. Logenthiran, Agent-based intelligent control for real-time operation of a microgrid, in: 2010 Joint International Conference on Power Electronics, Drives and Energy Systems 2010 Power India, 2010, pp. 1–6.

[20] F. Lopes, H. Algarvio, H. Coelho, Agent-based simulation of retail electricity markets: Bilateral trading players, in: 2013 24th International Workshop on Database and Expert Systems Applications, 2013, pp. 189–93.

[21] J. Yu, J.-Z. Zhou, J.-J. Yang, W. Wu, B. Fu, R.-T. Liao, Agent-based retail electricity market: modeling and analysis, in: Proceedings of 2004 International Conference on Machine Learning and Cybernetics (IEEE Cat. No.04EX826), Vol. 1, 2004, pp. 95–100.

[22] R. Yang, L. Wang, Development of multi-agent system for building energy and comfort management based on occupant behaviors, Energy and Buildings 56 (2013) 1–7.

[23] B. Kim, O. Lavrova, Two hierarchy (home and local) smart grid optimization by using demand response scheduling, in: 2013 IEEE PES Conference on Innovative Smart Grid Technologies (ISGT Latin America), 2013, pp. 1–8.

[24] T. Logenthiran, D. Srinivasan, A. M. Khambadkone, Multi-agent system for energy resource scheduling of integrated microgrids in a distributed system, Electric Power Systems Research 81 (1) (2011) 138–48.

[25] Y. Zhang, A. Lundblad, P. E. Campana, F. Benavente, J. Yan, Battery sizing and rule-based operation of grid-connected photovoltaic-battery system: A case study in sweden, Energy Conversion and Management 133 (2017) 249–63.

[26] R. Amirante, E. Cassone, E. Distaso, P. Tamburrano, Overview on recent developments in energy storage: Mechanical, electrochemical and hydrogen technologies, Energy Conversion and Management 132 (2017) 372–87.

[27] F. Rahimi, A. Ipakchi, F. Fletcher, The changing electrical landscape: End-to-end power system operation under the transactive energy paradigm, IEEE Power and Energy Magazine 14 (3) (2016) 52–62.

[28] K. Kok, S. Widergren, A society of devices: Integrating intelligent distributed resources with transactive energy, IEEE Power and Energy Magazine 14 (3) (2016) 34–45.

[29] A. Buonomano, F. Calise, A. Palombo, M. Vicidomini, Adsorption chiller operation by recovering low-temperature heat from building integrated photovoltaic thermal collectors: Modelling and simulation, Energy Conversion and Management (2017) –.

[30] J. Hu, G. Yang, H. W. Bindner, Y. Xue, Application of network-constrained transactive control to electric vehicle charging for secure grid operation, IEEE Transactions on Sustainable Energy PP (99) (2016) 1–1.

[31] D. Forfia, M. Knight, R. Melton, The view from the top of the mountain: Building a community of practice with the gridwise transactive energy framework, IEEE Power and Energy Magazine 14 (3) (2016) 25–33.

[32] L. Riboldi, L. O. Nord, Concepts for lifetime efficient supply of power and heat to offshore installations in the north sea, Energy Conversion and Management 148 (2017) 860–75.

[33] M. Marzband, E. Yousefnejad, A. Sumper, J. L. Domínguez-García, Real time experimental implementation of optimum energy management system in standalone microgrid by using multi-layer ant colony optimization, International Journal of Electrical Power & Energy Systems, 75 (2016) 265–74.

[34] M. Marzband, M. Javadi, J. L. Domínguez-García, M. M. Moghaddam, Non-cooperative game theory based energy management systems for energy district in the retail market considering DER uncertainties, IET Generation, Transmission & Distribution, 10 (2016) 2999–3009.

[35] M. Marzband, A. Sumper, A. Ruiz-Álvarez, J. L. Domínguez-García, B. Tomoiagă, Experimental evaluation of a real time energy management system for stand-alone microgrids in day-ahead markets, Applied Energy 106 (0) (2013) 365–76.

[36] M. Marzband, M. Ghadimi, A. Sumper, J. L. Domínguez-García, Experimental validation of a real-time energy management system using multi-period gravitational search algorithm for microgrids in islanded mode, Applied Energy, 128 (0) (2014) 164–74.

[37] G. Vyas, K. Jha, Benchmarking green building attributes to achieve cost effectiveness using a data envelopment analysis, Sustainable Cities and Society 28 (Supplement C) (2017) 127–34.

[38] M. Marzband, Experimental validation of optimal real-time energy management system for microgrids, Phd thesis, Departament d'Enginyeria Elèctrica,

EU d'Enginyeria Tècnica Industrial de Barcelona, Universitat Politècnica de Catalunya (2013).

[39] M. Marzband, H. Alavi, S. S. Ghazimirsaeid, H. Uppal, T. Fernando, Optimal energy management system based on stochastic approach for a home microgrid with integrated responsive load demand and energy storage, Sustainable Cities and Society, 28 (2017) 256–64.

[40] M. Marzband, F. Azarinejadian, M. Savaghebi, J. M. Guerrero, An optimal energy management system for islanded microgrids based on multiperiod artificial bee colony combined with markov chain, IEEE systems journal, PP (99) (2015) 1–11.

[41] M. Marzband, S. S. Ghazimirsaeid, H. Uppal, T. Fernando, A real-time evaluation of energy management systems for smart hybrid home microgrids, Electric Power Systems Research, 143 (2017) 624–33.

[42] J. Valinejad, M. Marzband, M. F. Akorede, T. Barforoshi, M. Jovanović, Generation expansion planning in electricity market considering uncertainty in load demand and presence of strategic GENCOs, Electric Power Systems Research 152 (2017) 92–104.

[43] M. Marzband, R. R. Ardeshiri, M. Moafi, H. Uppal, Distributed generation for economic benefit maximization through coalition formation based game theory concept, International Transactions on Electrical Energy Systems, (2017) 1–16.

[44] M. Marzband, M. M. Moghaddam, M. F. Akorede, G. Khomeyrani, Adaptive load shedding scheme for frequency stability enhancement in microgrids, Electric Power Systems Research, (2016) 1–11.

[45] A. Martinez, J.-H. Choi, Exploring the potential use of building facade information to estimate energy performance, Sustainable Cities and Society 35 (2017) 511–21.

[46] M. Marzband, A. Sumper, O. Gomis-Bellmunt, P. Pezzini, M. Chindris, Frequency control of isolated wind and diesel hybrid microgrid power system by using fuzzy logic controllers and PID controllers, in: Electrical Power Quality and Utilisation (EPQU), 2011 11th International Conference on, 2011, pp. 1–6.

[47] R. Banani, M. M. Vahdati, M. Shahrestani, D. Clements-Croome, The development of building assessment criteria framework for sustainable non-residential buildings in saudi arabia, Sustainable Cities and Society 26 (2016) 289–305.

[48] M. Marzband, N. Parhizi, J. Adabi, Optimal energy management for stand-alone microgrids based on multi-period imperialist competition algorithm considering uncertainties: experimental validation, International Transactions on Electrical Energy Systems, 30 (1) (2015) 122–31.

[49] J. Si, L. Marjanovic-Halburd, F. Nasiri, S. Bell, Assessment of building-integrated green technologies: A review and case study on applications of multi-criteria decision making (mcdm) method, Sustainable Cities and Society 27 (2016) 106–15.

[50] M. Marzband, N. Parhizi, M. Savaghebi, J. Guerrero, Distributed smart decision-making for a multimicrogrid system based on a hierarchical interactive architecture, IEEE Transactions on Energy Conversion, 31 (2) (2016) 637–48.

[51] M. Marzband, A. Sumper, Implementation of an optimal energy management within islanded microgrid, International Conference on Renewable Energies and Power Quality (ICREPQ), Cordoba, Spain, 2014.

[52] M. Marzband, A. Sumper, M. Chindriş, B. Tomoiagă, Energy management system of hybrid microgrid with energy storage, *The International Word Energy System Conference (WESC)*, Suceava, Romania, 2012.

[53] B. gang Hwang, M. Shan, N. N. B. Supaat, Green commercial building projects in singapore: Critical risk factors and mitigation measures, Sustainable Cities and Society 30 (2017) 237–47.

[54] M. Marzband, A. Sumper, J. L. Domínguez-García, R. Gumara-Ferret, Experimental validation of a real time energy management system for microgrids in islanded mode using a local day-ahead electricity market and MINLP, Energy Conversion and Management 76 (0) (2013) 314–22.

[55] M. Moafi, M. Marzband, M. Savaghebi, J. M. Guerrero, Energy management system based on fuzzy fractional order PID controller for transient stability improvement in microgrids with energy storage, International Transactions on Electrical Energy Systems (2016) 1–20.

[56] B. S. Y. Jin, Trade-off between performance and robustness: An evolutionary multiobjective approach, Springer Berlin Heidelberg (2003) 237–51.

[57] N. Parhizi, M. Marzband, S. M. M. Moghaddam, F. Azarinajadian, B. Mohamadi-Ivatlo, Optimal energy management system implementation in power networks with multiple microgrids by using multi-period imperialist competition, Comput. Intell. Electr. Eng.Accepted.

[58] R. Chatthaworn, S. Chaitusaney, Transmission network expansion planning considering renewable energy target with taguchi's orthogonal array testing, IEEJ Trans. Electr. Electron. Eng. 9 (2014) 588–99.

[59] H. Yu, C. Chung, K. Wong, Robust transmission network expansion planning method with taguchi's orthogonal array testing, IEEE Transactions on Power Systems, 26 (3) (2011) 1573–80.

[60] M. Bounou, S. Lefebvre, X. Do, Improving the quality of an optimal power flow solution by taguchi method, International Journal of Electrical Power & Energy Systems 17 (2) (1995) 113–18.

[61] M. Klusch, A. Gerber, Dynamic coalition formation among rational agents, Intelligent Systems, 17 (3) (2002) 42–7.

[62] E. Bonabeau, M. Dorigo, G. Theraulaz, in: Swarm Intelligence: From Natural to Artificial Systems, 1999, p. 320.

[63] J. J. Liang, A. K. Qin, P. N. Suganthan, S. Baskar, Comprehensive learning particle swarm optimizer for global optimization of multimodal functions, IEEE Transactions on Evolutionary Computation 10 (3) (2006) 281–295.

[64] W. feng Gao, S. yang Liu, L. ling Huang, Particle swarm optimization with chaotic opposition-based population initialization and stochastic search technique, Communications in Nonlinear Science and Numerical Simulation 17 (11) (2012) 4316–327.

[65] T. Robic, B. Filipi, in: DEMO: Differential Evolution for Multiobjective Optimization, 2005, pp. 520–33.

[66] S. Das, A. Abraham, A. Konar, Automatic clustering using an improved differential evolution algorithm, IEEE Transactions on Systems, Man, and Cybernetics- Part A: Systems and Humans 38 (1) (2008) 218–237.

[67] R. Storn, K. Price, Differential evolutio- a simple and efficient heuristic for global optimization over continuous spaces, J. of Global Optimization 11 (4) (1997) 341–359.

[68] A. Khazali, M. Kalantar, Optimal reactive power dispatch based on harmony search algorithm, International Journal of Electrical Power Energy Systems 33 (3) (2011) 684–92.

[69] Z. W. Geem, J. H. Kim, G. Loganathan, Optimal reactive power dispatch based on harmony search algorithm, SAGE Publications Ltd STM 76 (2) (2001) 60–68.

[70] S. Tuo, L. Yong, T. Zhou, An improved harmony search based on teaching-learning strategy for unconstrained optimization problems, Mathematical Problems in Engineering 2013 (2013) 1–30.

[71] X. S. Yang, A new metaheuristic bat-inspired algorithm, Stud. Comput. Intell. 76 (2) (2005) 65–74.

[72] Y. Zhou, L. Li, M. Ma, A complex-valued encoding bat algorithm for solving 0âĂŞ1 knapsack problem, SAGE Publications Ltd STM 44 (2) (2016) 407–30.

[73] M. Marzband, M. Javadi, S. A. Pourmousavi, G. Lightbody, An advanced retail electricity market for active distribution systems and home microgrid interoperability based on game theory, Electric Power Systems Research 157 (2018) 187–99.

[74] R. Billinton, a. Bonaert, a. Koivo, Power System Reliability Evaluation, 5th Edition, Vol. 1, Gordon and Breach, New York, 1971.

[75] M. Fotuhi-Firuzabad, M. Rastegar, A. Safdarian, F. Aminifar, Probabilistic home load controlling considering plug-in hybrid electric vehicle uncertainties, in: Reliability Modeling and Analysis of Smart Power Systems, Springer India, 2014, pp. 117–32.

[76] A. Daniel, A. Chen, Stochastic simulation and forecasting of hourly average wind speed sequences in jamaica, Solar Energy, 46 (1) (1991) 1–11.

[77] B. Borowy, Z. Salameh, Optimum photovoltaic array size for a hybrid wind/PV system, IEEE Transactions on Energy Conversion, 9 (3) (1994) 482–88.

[78] G. Tina, S. Gagliano, S. Raiti, Hybrid solar/wind power system probabilistic modelling for long-term performance assessment, Solar Energy, 80 (5) (2006) 578–88.

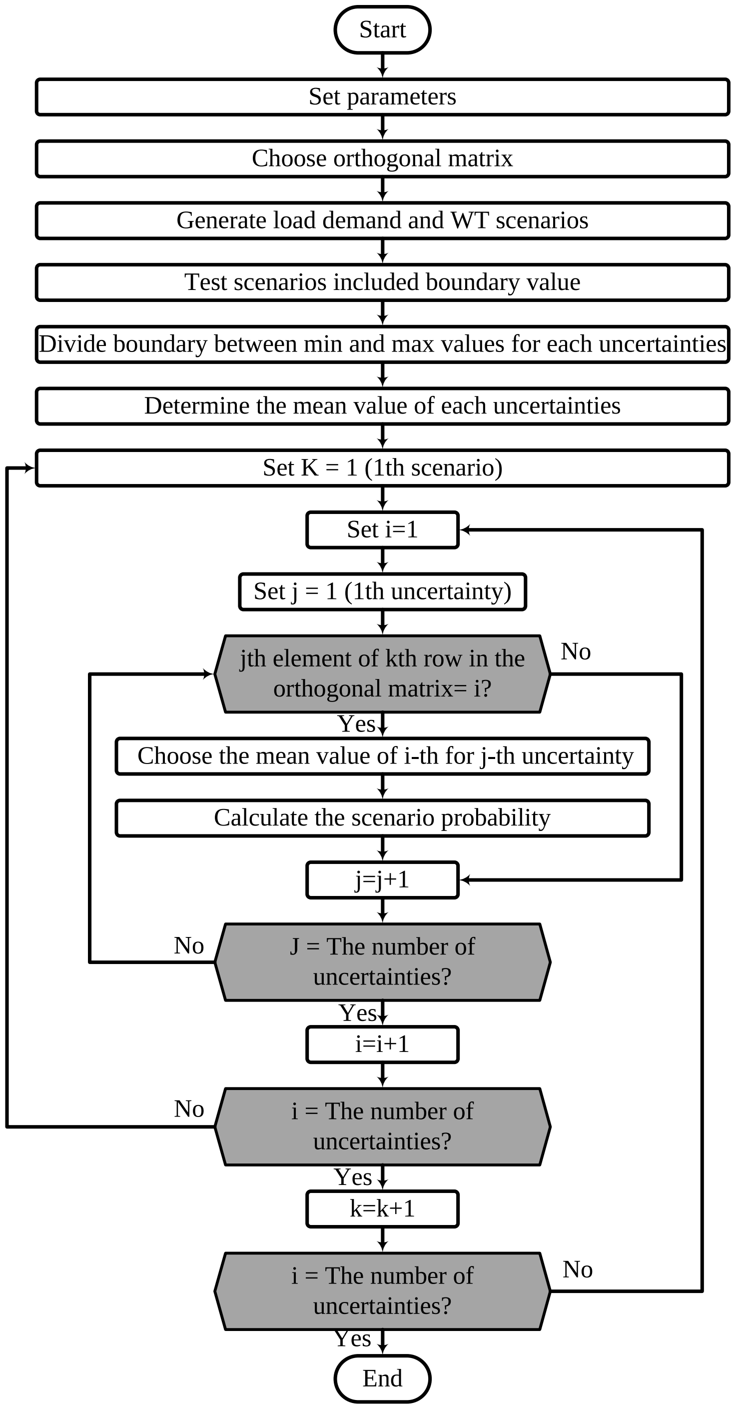

Figure 3: Uncertainty unit based on TOAT method

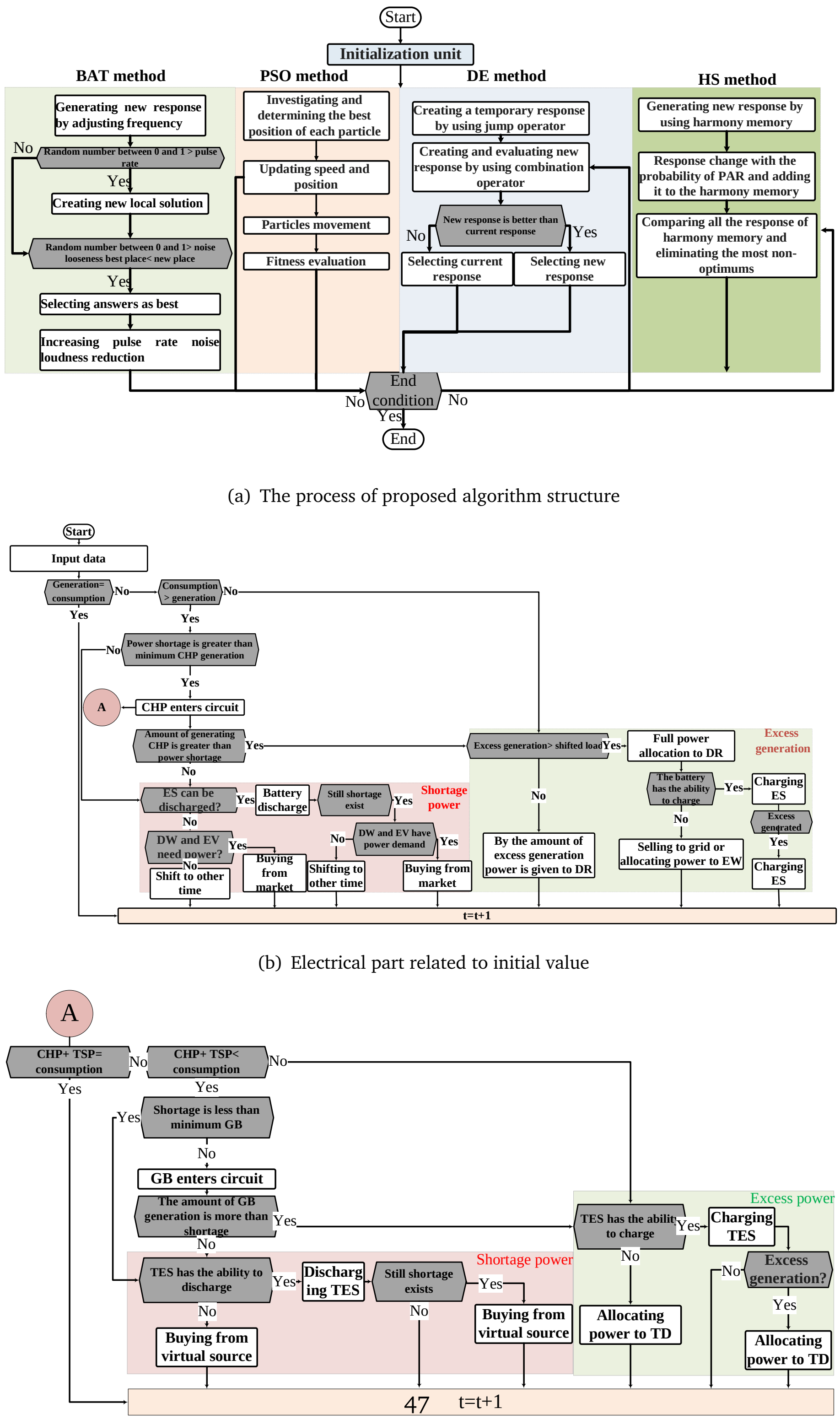

(a) The process of proposed algorithm structure

(b) Electrical part related to initial value

(c) Thermal part related to initial value

Figure 4: The proposed flowchart for the TE unit

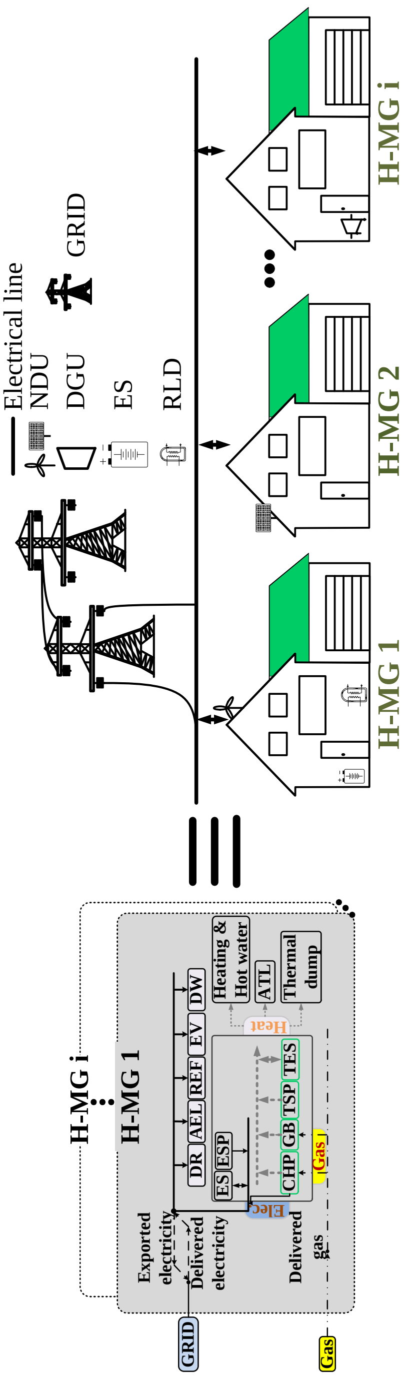

Figure 5: The schematic of neighbourhood system with several H-MGs (solid black lines show the electrical part, gray dash shows the thermal part and the dash-point is related to gas branch)

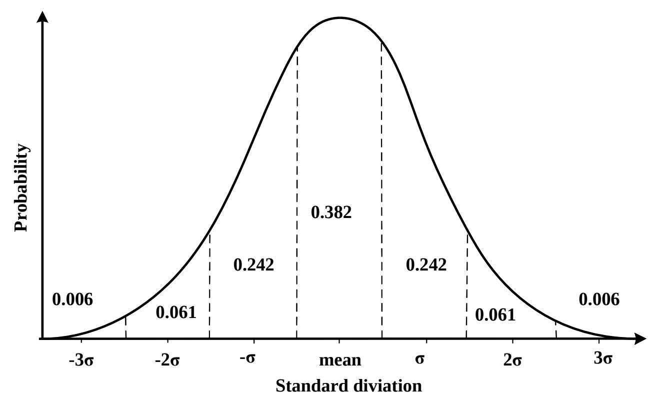

Figure 6: Seven-segment normal probability distribution curve

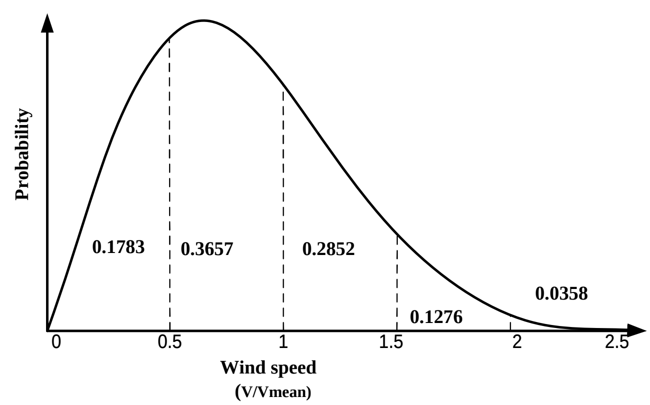

Figure 7: Wind speed probability distribution

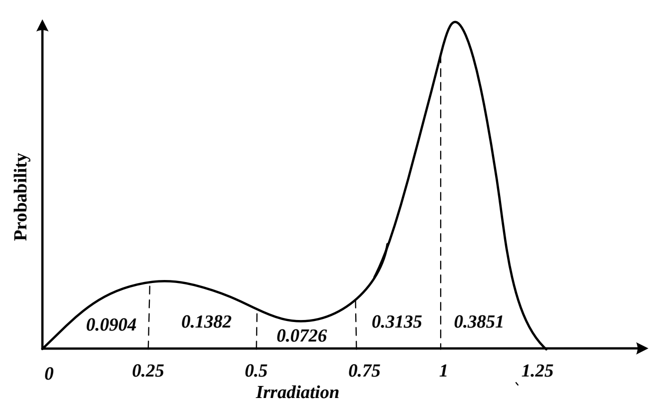

Figure 8: Solar radiation probabilistic distribution

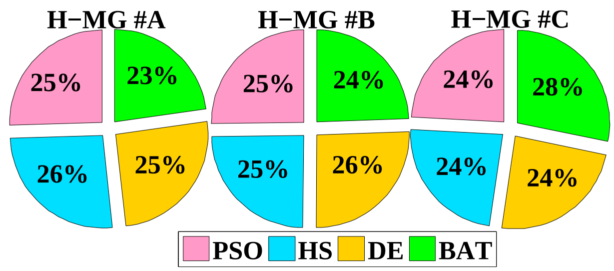

(a) The total generated power in each H-MG

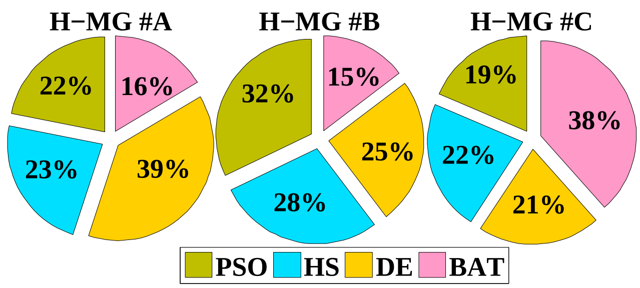

(b) The electrical power sold by the H-MGs to the retailers

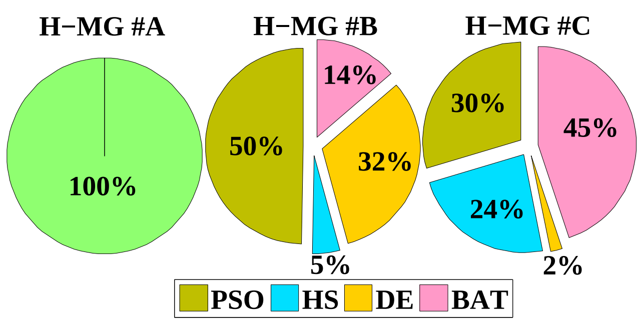

(c) The electrical power bought by the H-MGs from the retailers

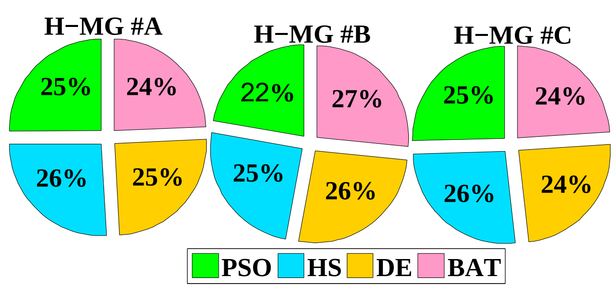

(d) The total generated thermal power in each H-MG

Figure 9: The electrical and thermal powers consumed by each H-MG using different optimization methods

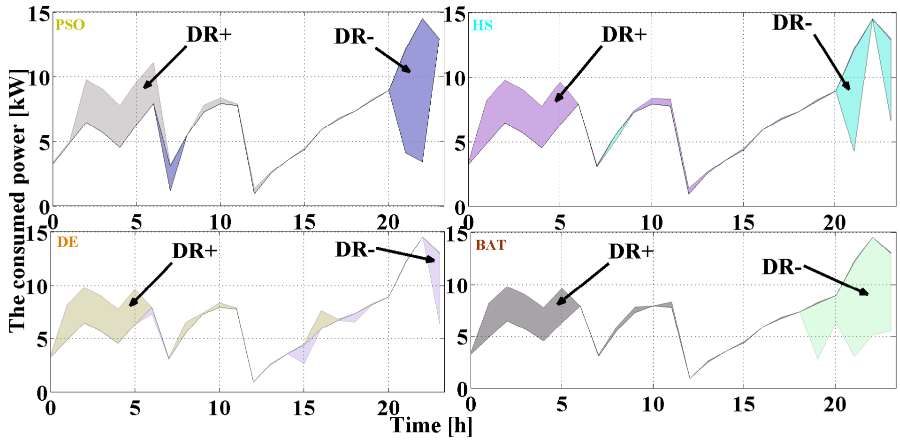

(a) H-MG #A

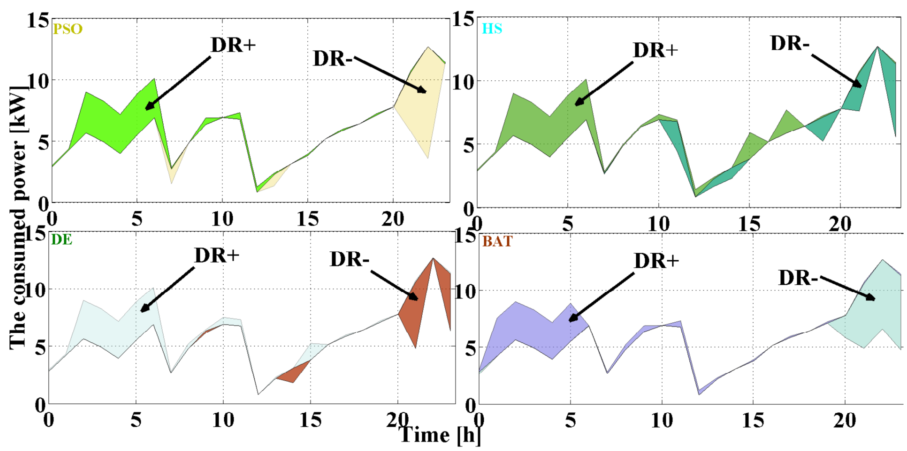

(b) H-MG #B

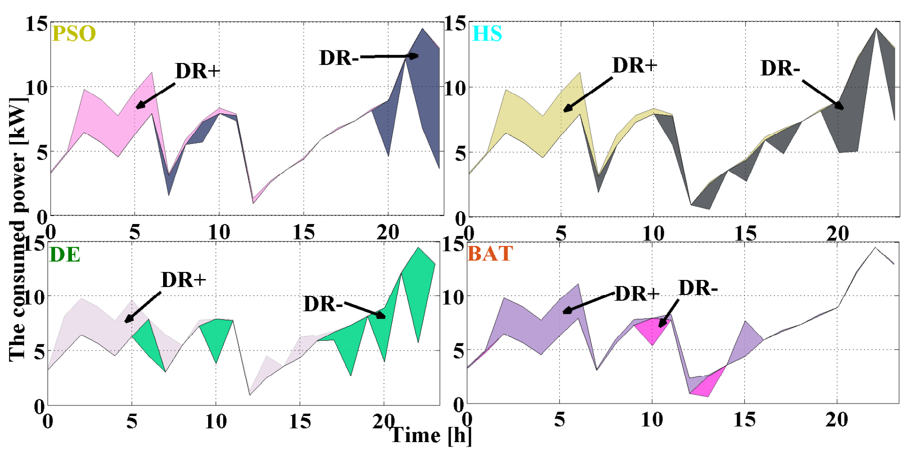

(c) H-MG #C

Figure 10: The consumed load demand profile in the H-MGs

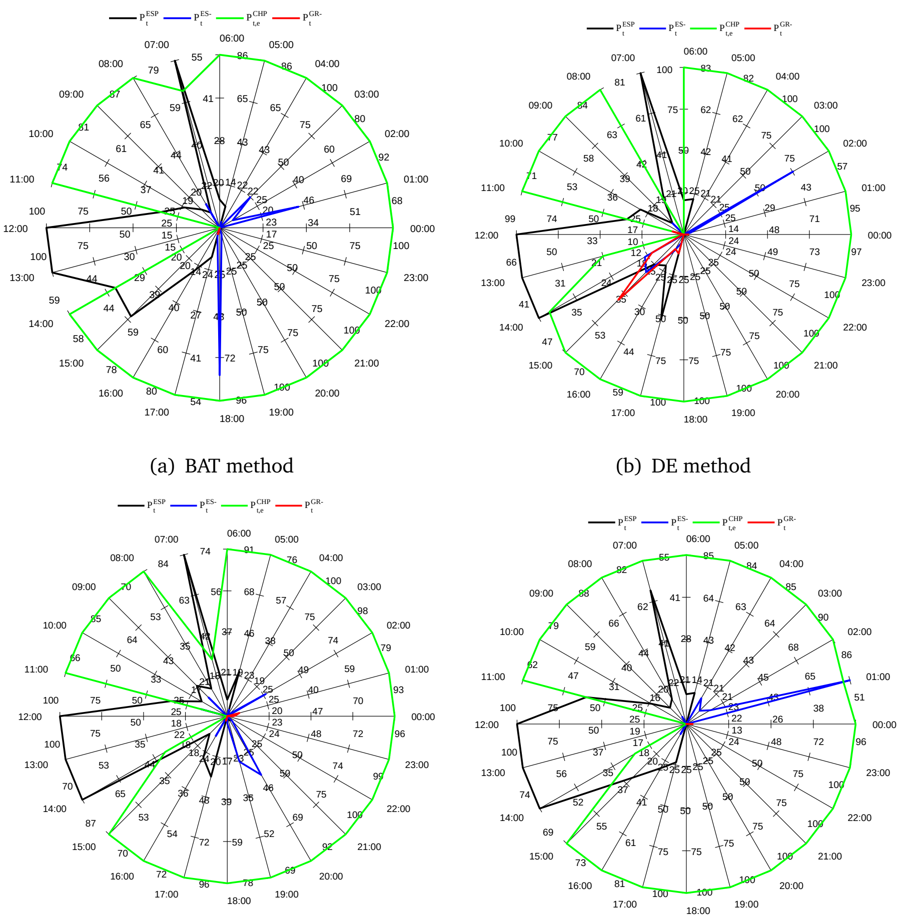

(a) BAT method

(b) DE method

(c) HS method

(d) PSO method

Figure 11: Electrical power percentage generated by the generation resources existing in the H-MGs based on BAT, DE, HS and PSO algorithms

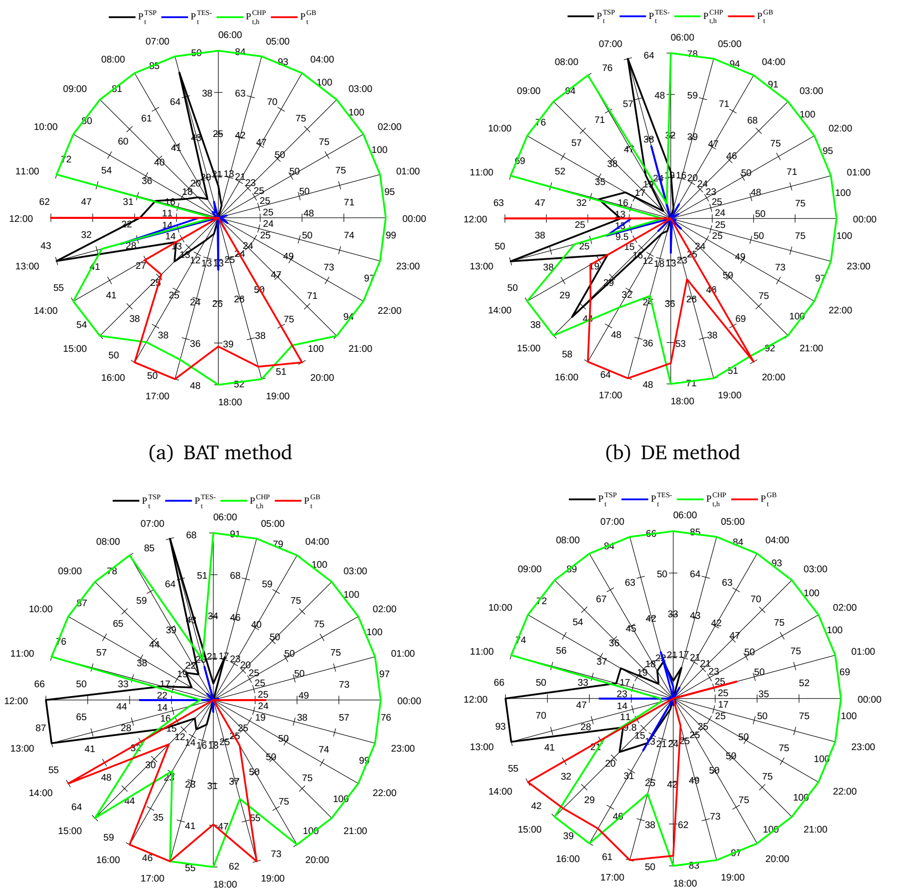

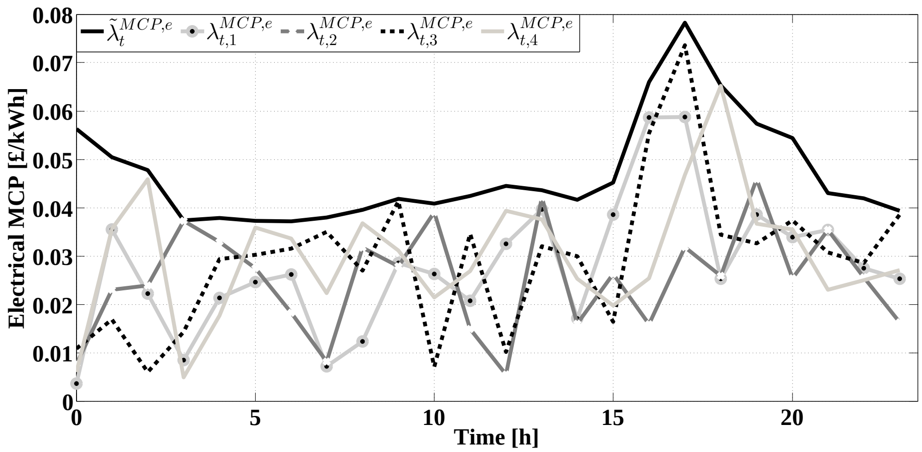

(a) Electrical MCP

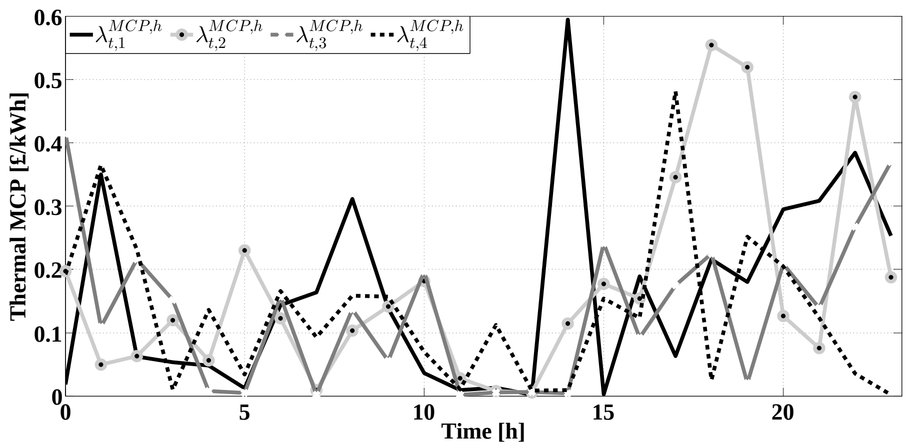

(b) Thermal MCP

Figure 13: MCP profile for the 24h performance of the system under study using different optimization methods

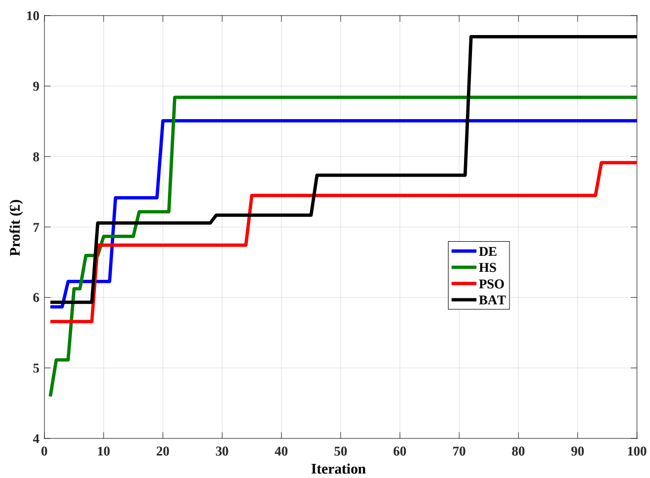

Figure 14: Convergence characteristics of the proposed algorithms